Structural Engineering and Mechanics, *Vol. 57, No. 3 (2016) 473-506*
DOI: http://dx.doi.org/10.12989/sem.2016.57.3.473

Development of a 2D isoparametric finite element model based on the layerwise approach for the bending analysis of sandwich plates

Mohamed-Ouejdi Belarbi[a], Abdelouahab Tati[b], Houdayfa Ounis[c] and Adel Benchabane*

Laboratoire de Génie Energétique et Matériaux, LGEM. Université de Biskra, B.P. 145, R.P. 07000, Biskra, Algeria

(Received May 24, 2014, Revised January 5, 2015, Accepted January 11, 2016)

Abstract. The aim of this work is the development of a 2D quadrilateral isoparametric finite element model, based on a layerwise approach, for the bending analysis of sandwich plates. The face sheets and the core are modeled individually using, respectively, the first order shear deformation theory and the third-order plate theory. The displacement continuity condition at the interfaces 'face sheets-core' is satisfied. The assumed natural strains method is introduced to avoid an eventual shear locking phenomenon. The developed element is a four-nodded isoparametric element with fifty two degrees-of-freedom (52 DOF). Each face sheet has only two rotational DOF per node and the core has nine DOF per node: six rotational degrees and three translation components which are common for the all sandwich layers. The performance of the proposed element model is assessed by six examples, considering symmetric/unsymmetric composite sandwich plates with different aspect ratios, loadings and boundary conditions. The numerical results obtained are compared with the analytical solutions and the numerical results obtained by other authors. The results indicate that the proposed element model is promising in terms of the accuracy and the convergence speed for both thin and thick plates.

Keywords: layerwise; finite element; sandwich plates; bending

1. Introduction

Nowadays, composite sandwich structures gained considerable attention and became increasingly important in various areas of technology such as civil construction, marine industry and aerospace engineering due to their rigidity-and-resistance to weight ratios. However, there are still questions on the complexity of the behavior of these structures. The effect of shear deformation is quite significant which may lead to failure and becomes more complex in case of sandwich construction, as the material property variation is very large between the core and face

*Corresponding author, Professor, E-mail: adel.benchabane@gmail.com; a.benchabane@univ-biskra.dz
[a]Ph.D., E-mail: Belarbi.m.w@gmail.com
[b]Ph.D., E-mail: abdeltati@yahoo.fr
[c]Ph.D., E-mail: houdayfa.ounis@gmail.com

http://www.techno-press.org/?journal=sem&subpage=8 ISSN: 1225-4568 (Print), 1598-6217 (Online)

layers (Khandelwal *et al*. 2013). Moreover, an accurate estimation of stress components, specifically the transverse shear stresses, plays an important role in reducing these failures (Kant and Swaminathan 2000).

Several theories have been proposed to study the behavior of composite sandwich structures. Three different approaches can be distinguish: (i) The Three-Dimensional (3D), elasticity approach, (ii) The Equivalent Single Layer approach (ESL) and (iii) The Layerwise approach (LW) and Zig-Zag, (ZZT), theories.

The 3D elasticity approach, give very accurate results, but few authors adopted it, the fact that, high cost in computation time (Kant and Swaminathan 2002, Noor and Burton 1990, Pagano 1969, 1970, Srinivas and Rao 1971).

In the second approach, ESL approach, the heterogeneous multilayer plate is treated as a single equivalent homogeneous layer. This approach is the most adopted by researchers and can be divided into three major theories, namely: (1) the classical laminated plate theory (CLPT) which does not include the effect of the transverse shear deformation (Kirchhoff 1850, Librescu 1975, Ounis *et al*. 2014, Stavsky 1965, Whitney 1970); (2) the first order shear deformation theory (FSDT) where the effect of the transverse shear deformation is considered, but taken constant through the thickness (Kabir 1995, Reddy *et al*. 1987, Reissner 1975, Whitney and Pagano 1970); and (3) the higher order shear deformation theories (HSDT), where a better representation of transverse shear effect can be obtained (Aydogdu 2009, Grover *et al*. 2013, Kant 1982, Lo *et al*. 1977b,a, Manjunatha and Kant 1993, Nayak *et al*. 2003, Reddy 1984, Rezaiee-Pajand *et al*. 2012, Sheikh and Chakrabarti 2003, Tu *et al*. 2010, Kant and Kommineni 1992).

However, the ESL approach is unable to predict accurately the local behavior (e.g., interlaminar stresses) of sandwich structures. For that reason, many researchers developed more accurate theories such as zig–zag theories (Chakrabarti and Sheikh (2004, 2005), Kapuria and Kulkarni 2007, Nemeth 2012, Pandit *et al*. 2008, 2010, Singh *et al*. 2011, Topdar *et al*. 2003, Xiaohui *et al*. 2012, Sahoo and Singh 2013, Carrera 2003, Cho and Parmerter 1992, 1993, Di Sciuva1986, Murakami 1986, Khandelwal *et al*. 2013, Chalak *et al*. 2012, 2014) and layerwise approach (Lee and Fan 1996, Linke *et al*. 2007, Mantari *et al*. 2012, Oskooei and Hansen 2000, Plagianakos and Saravanos 2009, Ramesh *et al*. 2009, Ramtekkar *et al*. 2002, 2003, Reddy 1987, Robbins *et al*. 2005, Spilker 1982, Wu and Hsu 1993, Wu and Lin 1993, Ćetković and Vuksanović 2009, Kheirikhah *et al*. 2012, Maturi *et al*. 2014). This latter approach assume separate displacement field expansions within each material layer, thus providing a kinematically correct representation of the strain field in discrete laminated layer, and allowing accurate determination of ply level stresses (Reddy 1993). Survey of various researches on approaches, theories and finite elements models, can be found in references (Carrera 2002, Ha 1990, Khandan *et al*. 2012, Noor *et al*. 1996, Reddy and Robbins 1994, Zhang and Yang 2009).

In the literature, many researchers have adopted the layerwise approach to the development of finite elements, which are able to give a good description of sandwich structures. Wu and Lin (1993) presented a two-dimensional mixed finite element based on higher order layerwise model for the analysis of thick sandwich plates, where the displacement continuity at the interface is satisfied as well as the interlaminar stresses. These authors proposed for each layer a cubic and quadratic polynomial functions for in-plane and transverse displacements, respectively. Afterwards, Lee and Fan (1996) describe a new model in which, the first order shear deformation theory is used for the face sheets whereas the displacement at the core are expressed in terms of the two face sheets displacements. In this model, the transverse shear strain varies linearly while the transverse normal strain is constant through the thickness of the core. They used a nine-nodded isoparametric finite element to study the bending and vibration of sandwich plates. On the other hand, Oskooei and Hansen (2000) developed a three-dimensional finite element based on a layerwise model to analyze the sandwich plates with laminated face sheets. They used the first order shear deformation theory for the face sheets, whereas for the core a cubic and quadratic, functions for the in-plane and transverse, displacements, was adopted. In addition, an eighteen-nodes three-dimensional brick mixed finite element with six DOF at each node based on layerwise has been developed by Ramtekkar *et al*. (2002, 2003) for an accurate evaluation of transverse stresses in laminated sandwich. The continuity of displacements as well as the transverse stresses is satisfied. In the same context, Linke *et al*. (2007) developed a three-dimensional displacement finite element containing eleven DOF at each node (each face sheet contains five DOF per node and only one DOF in the core) for static and stability analysis of sandwich plates. The formulation of this element is based on the layerwise approach, where the face sheets are represented as an elements of classical plate theory and the core is represented by the third order shear deformation theory. The in and out-of, plane displacements of the core assume a cubic and quadratic variation, respectively. Recently, Mantari *et al*. (2012) presented a new layerwise model using a trigonometric displacement field for in-plane displacements and constant out-of plane displacements through the thickness. The authors used a C^0 four- node isoparametric quadrilateral element in order to study the bending of thick sandwich panels.

In this work, a new layerwise finite element model has been developed for the bending analysis of sandwich plates. The face sheets are modeled based on the first order shear deformation theory, whereas the core is modeled using the third-order shear deformation plate theory. Several examples have been examined, for symmetric/unsymmetric composite laminated, sandwich and skew plates, in order to test the performance and the convergence of the developed element model. Thus, the obtained numerical results can be compared with the analytical solutions and the numerical results found in literature.

2. Mathematical model

Sandwich plate is a structure composed of three principal layers as shown in (Fig. 1): two face sheets (top-bottom) of thicknesses (h_t), (h_b) respectively, and a central layer named core of thickness (h_c) which is thicker than the previous ones. Total thickness (h) of the plate is the sum of these thicknesses. The plane (x,y) coordinate system coincides with mi-plane plate.

2.1 Kinematics

In the present layerwise model, the core is modeled using the third order shear deformation plate theory (TSDT), whereas the first order shear deformation theory (FSDT) is adopted for the two face sheets.

• *Core*

The displacement field for the core is written as a third-order Taylor series expansion of the in-plane displacements in the thickness coordinate, and as a constant one for the transverse displacement

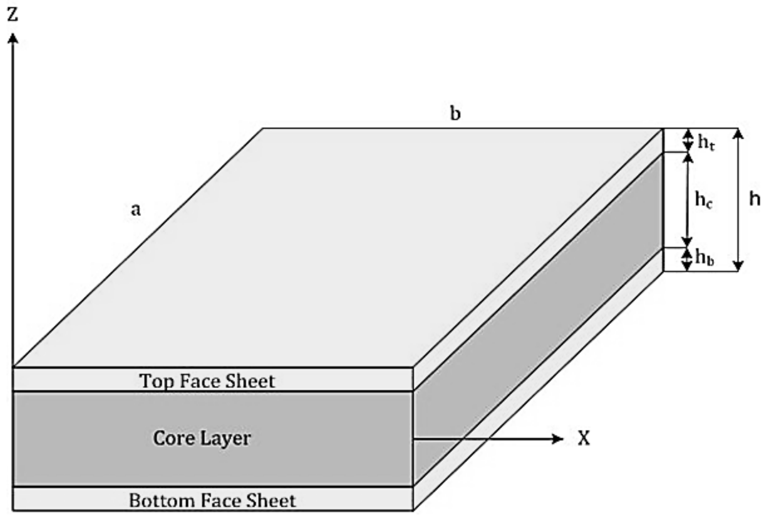

Fig. 1 Geometry and notations of a sandwich plate

$$
\begin{aligned}
u_c &= u_0 + Z\psi_x^c + Z^2\eta_x^c + Z^3\zeta_x^c \\
v_c &= v_0 + Z\psi_y^c + Z^2\eta_y^c + Z^3\zeta_y^c \\
w_c &= w_0
\end{aligned}
\tag{1}
$$

where u_0, v_0 and w_0 are respectively, in-plane and transverse displacement components at the mid-plane of the sandwich plate. ψ_x^c , ψ_y^c represent normal rotations about the x and y axis respectively. η_x^c, η_y^c, ζ_x^c and ζ_y^c are higher order terms.

• *Top face sheet*

The compatibility conditions as well as the displacement continuity at the interface (top face sheet-core-bottom face sheet), leads to the following improved displacement fields (Fig. 2)

$$
\begin{aligned}
u_t &= u_c\left(\frac{h_c}{2}\right) + \left(Z - \frac{h_c}{2}\right)\psi_x^t \\
v_t &= v_c\left(\frac{h_c}{2}\right) + \left(Z - \frac{h_c}{2}\right)\psi_y^t \\
w_t &= w_0
\end{aligned}
\tag{2}
$$

where ψ_x^t and ψ_y^t are the rotations of the top face-sheet cross section about the y and x axis, respectively.

with

$$
\begin{aligned}
u_c\left(\frac{h_c}{2}\right) &= u_0 + \left(\frac{h_c}{2}\right)\psi_x^c + \left(\frac{h_c^2}{4}\right)\eta_x^c + \left(\frac{h_c^3}{8}\right)\zeta_x^c \\
v_c\left(\frac{h_c}{2}\right) &= v_0 + \left(\frac{h_c}{2}\right)\psi_y^c + \left(\frac{h_c^2}{4}\right)\eta_y^c + \left(\frac{h_c^3}{8}\right)\zeta_y^c
\end{aligned}
\tag{3}
$$

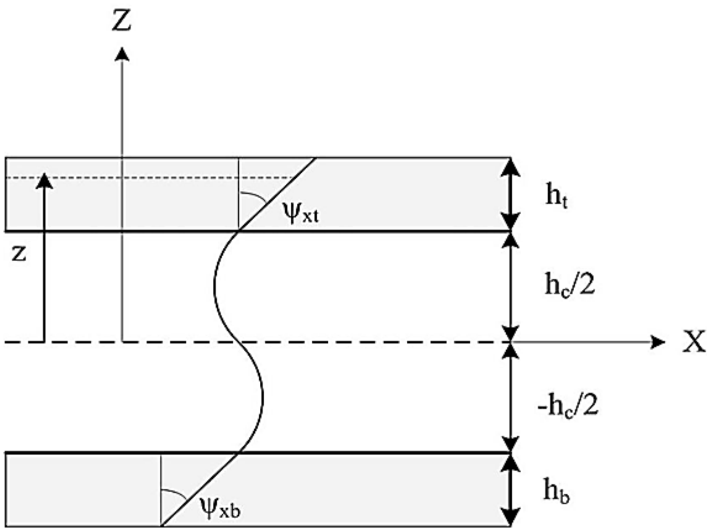

Fig. 2 Kinematics of QSFT52 model

The substitution of Eq. (3) in Eq. (2) led finally to the following expressions

$$\begin{aligned}
u_t &= u_0 + \left(\frac{h_c}{2}\right)\psi_x^c + \left(\frac{h_c^2}{4}\right)\eta_x^c + \left(\frac{h_c^3}{8}\right)\zeta_x^c + \left(Z - \frac{h_c}{2}\right)\psi_x^t \\
v_t &= v_0 + \left(\frac{h_c}{2}\right)\psi_y^c + \left(\frac{h_c^2}{4}\right)\eta_y^c + \left(\frac{h_c^3}{8}\right)\zeta_y^c + \left(Z - \frac{h_c}{2}\right)\psi_y^t \\
w_t &= w_0
\end{aligned} \tag{4}$$

• *Bottom face sheet*

According to Fig. 2, the displacement field of the bottom face sheet can be written as

$$\begin{aligned}
u_b &= u_c\left(-\frac{h_c}{2}\right) + \left(Z + \frac{h_c}{2}\right)\psi_x^b \\
v_b &= v_c\left(-\frac{h_c}{2}\right) + \left(Z + \frac{h_c}{2}\right)\psi_y^b \\
w_b &= w_0
\end{aligned} \tag{5}$$

where ψ_x^b and ψ_y^b are the rotations of the bottom face-sheet cross section about the y and x axis respectively

where

$$\begin{aligned}
u_c\left(-\frac{h_c}{2}\right) &= u_0 - \left(\frac{h_c}{2}\right)\psi_x^c + \left(\frac{h_c^2}{4}\right)\eta_x^c - \left(\frac{h_c^3}{8}\right)\zeta_x^c \\
v_c\left(-\frac{h_c}{2}\right) &= v_0 - \left(\frac{h_c}{2}\right)\psi_y^c + \left(\frac{h_c^2}{4}\right)\eta_y^c - \left(\frac{h_c^3}{8}\right)\zeta_y^c
\end{aligned} \tag{6}$$

Substituting of Eq. (6) in Eq. (5), the displacement field of the bottom face sheet is given by

$$\begin{aligned} u_b &= u_0 - \left(\frac{h_c}{2}\right)\psi_x^c + \left(\frac{h_c^2}{4}\right)\eta_x^c - \left(\frac{h_c^3}{8}\right)\zeta_x^c + \left(Z + \frac{h_c}{2}\right)\psi_x^b \\ v_b &= v_0 - \left(\frac{h_c}{2}\right)\psi_y^c + \left(\frac{h_c^2}{4}\right)\eta_y^c - \left(\frac{h_c^3}{8}\right)\zeta_y^c + \left(Z + \frac{h_c}{2}\right)\psi_y^b \\ w_b &= w_0 \end{aligned} \tag{7}$$

2.1.1 Strain-displacement relationships

The strain-displacement relationships derived from the displacement model of Eqs. (1), (4) and (7) are given as follows:

For the core layer,

$$\begin{aligned} \varepsilon_{xx}^c &= \frac{\partial u_0}{\partial x} + z\frac{\partial \psi_x^c}{\partial x} + z^2\frac{\partial \eta_x^c}{\partial x} + z^3\frac{\partial \zeta_x^c}{\partial x} \\ \varepsilon_{yy}^c &= \frac{\partial v_0}{\partial y} + z\frac{\partial \psi_y^c}{\partial y} + z^2\frac{\partial \eta_y^c}{\partial y} + z^3\frac{\partial \zeta_y^c}{\partial y} \\ \gamma_{xy}^c &= \left(\frac{\partial u_0}{\partial y} + \frac{\partial v_0}{\partial x}\right) + z\left(\frac{\partial \psi_x^c}{\partial y} + \frac{\partial \psi_y^c}{\partial x}\right) + z^2\left(\frac{\partial \eta_x^c}{\partial y} + \frac{\partial \eta_y^c}{\partial x}\right) + z^3\left(\frac{\partial \zeta_x^c}{\partial y} + \frac{\partial \zeta_y^c}{\partial x}\right) \\ \gamma_{yz}^c &= \psi_y^c + \frac{\partial w_0}{\partial y} + z2\eta_y^c + z^2 3\zeta_y^c \\ \gamma_{xz}^c &= \psi_x^c + \frac{\partial w_0}{\partial x} + z2\eta_x^c + z^2 3\zeta_x^c \end{aligned} \tag{8}$$

For the top face sheet

$$\begin{aligned} \varepsilon_{xx}^t &= \frac{\partial u_t}{\partial x} = \frac{\partial u_0}{\partial x} + \left(\frac{h_c}{2}\right)\frac{\partial \psi_x^c}{\partial x} + \left(\frac{h_c^2}{4}\right)\frac{\partial \eta_x^c}{\partial x} + \left(\frac{h_c^3}{8}\right)\frac{\partial \zeta_x^c}{\partial x} + (z - \frac{h_c}{2})\frac{\partial \psi_x^t}{\partial x} \\ \varepsilon_{yy}^t &= \frac{\partial v_t}{\partial y} = \frac{\partial v_0}{\partial x} + \left(\frac{h_c}{2}\right)\frac{\partial \psi_y^c}{\partial y} + \left(\frac{h_c^2}{4}\right)\frac{\partial \eta_y^c}{\partial y} + \left(\frac{h_c^3}{8}\right)\frac{\partial \zeta_y^c}{\partial y} + (z - \frac{h_c}{2})\frac{\partial \psi_y^t}{\partial y} \\ \gamma_{xy}^t &= \frac{\partial u_t}{\partial y} + \frac{\partial v_t}{\partial x} = \left(\frac{\partial u_0}{\partial y} + \frac{\partial v_0}{\partial x}\right) + \frac{h_c}{2}\left(\frac{\partial \psi_x^c}{\partial y} + \frac{\partial \psi_y^c}{\partial x}\right) + \frac{h_c^2}{4}\left(\frac{\partial \eta_x^c}{\partial y} + \frac{\partial \eta_y^c}{\partial x}\right) \\ &\quad + \frac{h_c^3}{8}\left(\frac{\partial \zeta_x^c}{\partial y} + \frac{\partial \zeta_y^c}{\partial x}\right) + (z - \frac{h_c}{2})\left(\frac{\partial \psi_x^t}{\partial y} + \frac{\partial \psi_y^t}{\partial x}\right) \\ \gamma_{yz}^t &= \frac{\partial w_0}{\partial y} + \psi_y^t \\ \gamma_{xz}^t &= \frac{\partial w_0}{\partial x} + \psi_x^t \end{aligned} \tag{9}$$

For the bottom face sheet

$$\varepsilon_{xx}^{b}=\frac{\partial u_b}{\partial x}=\frac{\partial u_0}{\partial x}-\left(\frac{h_c}{2}\right)\frac{\partial \psi_x^c}{\partial x}+\left(\frac{h_c^2}{4}\right)-\frac{\partial \eta_x^c}{\partial x}\left(\frac{h_c^3}{8}\right)\frac{\partial \zeta_x^c}{\partial x}+(z+\frac{h_c}{2})\frac{\partial \psi_x^b}{\partial x}$$

$$\varepsilon_{yy}^{b}=\frac{\partial v_b}{\partial y}=\frac{\partial v_0}{\partial y}-\left(\frac{h_c}{2}\right)\frac{\partial \psi_y^c}{\partial y}+\left(\frac{h_c^2}{4}\right)-\frac{\partial \eta_y^c}{\partial y}\left(\frac{h_c^3}{8}\right)\frac{\partial \zeta_y^c}{\partial y}+(z+\frac{h_c}{2})\frac{\partial \psi_y^b}{\partial y}$$

$$\gamma_{xy}^{b}=\frac{\partial u_b}{\partial y}+\frac{\partial v_b}{\partial x}=\left(\frac{\partial u_0}{\partial y}+\frac{\partial v_0}{\partial x}\right)-\frac{h_c}{2}\left(\frac{\partial \psi_x^c}{\partial y}+\frac{\partial \psi_y^c}{\partial x}\right)+\frac{h_c^2}{4}\left(\frac{\partial \eta_x^c}{\partial y}+\frac{\partial \eta_y^c}{\partial x}\right)$$

$$-\frac{h_c^3}{8}\left(\frac{\partial \zeta_x^c}{\partial y}+\frac{\partial \zeta_y^c}{\partial x}\right)+(z+\frac{h_c}{2})\left(\frac{\partial \psi_x^b}{\partial y}+\frac{\partial \psi_y^b}{\partial x}\right)$$

$$\gamma_{yz}^{b}=\frac{\partial w_0}{\partial y}+\psi_y^b$$

$$\gamma_{xz}^{b}=\frac{\partial w_0}{\partial x}+\psi_x^b \tag{10}$$

2.2 Constitutive relationships

In this work, the two face sheets (top and bottom) are considered as laminated composite. Hence, the stress-strain relationship of the k^{th} layer in the global coordinate system is given as

$$\begin{Bmatrix}\sigma_x^f\\ \sigma_y^f\\ \tau_{yz}^f\\ \tau_{xz}^f\\ \tau_{xy}^f\end{Bmatrix}_{(k)}=\begin{bmatrix}\overline{Q_{11}} & \overline{Q_{12}} & 0 & 0 & \overline{Q_{16}}\\ \overline{Q_{21}} & \overline{Q_{22}} & 0 & 0 & \overline{Q_{26}}\\ 0 & 0 & \overline{Q_{44}} & \overline{Q_{45}} & 0\\ 0 & 0 & \overline{Q_{54}} & \overline{Q_{55}} & 0\\ \overline{Q_{61}} & \overline{Q_{62}} & 0 & 0 & \overline{Q_{66}}\end{bmatrix}_{(k)}\begin{Bmatrix}\varepsilon_{xx}^f\\ \varepsilon_{yy}^f\\ \gamma_{yz}^f\\ \gamma_{xz}^f\\ \gamma_{xy}^f\end{Bmatrix}_{(k)};\quad f\text{=top, bottom} \tag{11}$$

The core is considered as an orthotropic composite material and the stress-strain relationship is given by

$$\begin{Bmatrix}\sigma_{xx}\\ \sigma_{yy}\\ \tau_{yz}\\ \tau_{xz}\\ \sigma_{xy}\end{Bmatrix}=\begin{bmatrix}\overline{Q_{11}} & \overline{Q_{12}} & 0 & 0 & \overline{Q_{16}}\\ \overline{Q_{21}} & \overline{Q_{22}} & 0 & 0 & \overline{Q_{26}}\\ 0 & 0 & \overline{Q_{44}} & \overline{Q_{45}} & 0\\ 0 & 0 & \overline{Q_{54}} & \overline{Q_{55}} & 0\\ \overline{Q_{61}} & \overline{Q_{62}} & 0 & 0 & \overline{Q_{66}}\end{bmatrix}\begin{Bmatrix}\varepsilon_{xx}\\ \varepsilon_{yy}\\ \gamma_{yz}\\ \gamma_{xz}\\ \gamma_{xy}\end{Bmatrix} \tag{12}$$

The stress resultants of the core are calculated by integration of the stresses through the thickness direction of laminated plate as follows

$$\begin{bmatrix} N_x & M_x & \overline{N_x} & \overline{M_x} \\ N_y & M_y & \overline{N_y} & \overline{M_y} \\ N_{xy} & M_{xy} & \overline{N_{xy}} & \overline{M_{xy}} \end{bmatrix} = \int_{-\frac{h}{2}}^{\frac{h}{2}} \begin{Bmatrix} \sigma_x \\ \sigma_y \\ \tau_{xy} \end{Bmatrix} \left(1, z, z^2, z^3\right) dz \tag{13a}$$

$$\begin{bmatrix} V_x & S_x & R_x \\ V_y & S_y & R_y \end{bmatrix} = \int_{-\frac{h}{2}}^{\frac{h}{2}} \begin{Bmatrix} \tau_{xz} \\ \tau_{yz} \end{Bmatrix} \left(1, z, z^2\right) dz \tag{13b}$$

where N, M, $\overline{N}$ and $\overline{M}$, denote membrane, bending moment, higher order membrane and higher order moment resultants respectively. V is the shear resultant; S and R are the higher order shear resultant.

By introducing the constitutive equation in the expressions of the resultant stress, (13a), (13b) the generalized constitutive equations become

$$\begin{Bmatrix} N \\ M \\ \overline{N} \\ \overline{M} \end{Bmatrix} = \begin{bmatrix} [A] & [B] & [D] & [E] \\ [B] & [D] & [E] & [F] \\ [D] & [E] & [F] & [G] \\ [E] & [F] & [G] & [H] \end{bmatrix} \begin{Bmatrix} \varepsilon^{(0)} \\ \chi^{(1)} \\ \chi^{(2)} \\ \chi^{(3)} \end{Bmatrix} \tag{14a}$$

$$\begin{Bmatrix} V \\ S \\ R \end{Bmatrix} = \begin{bmatrix} [A^s] & [B^s] & [D^s] \\ [B^s] & [D^s] & [E^s] \\ [D^s] & [E^s] & [F^s] \end{bmatrix} \begin{Bmatrix} \gamma_s^{(0)} \\ \chi_s^{(1)} \\ \chi_s^{(2)} \end{Bmatrix} \tag{14b}$$

where $N = \left(N_x \quad N_y \quad N_{xy}\right)^T$, $M = \left(M_x \quad M_y \quad M_{xy}\right)^T$, $\overline{N} = \left(\overline{N_x} \quad \overline{N_y} \quad \overline{N_{xy}}\right)^T$,

$\overline{M} = \left(\overline{M_x} \quad \overline{M_y} \quad \overline{M_{xy}}\right)^T$, $V = \left(V_x \quad V_y\right)^T$, $S = \left(S_x \quad S_y\right)^T$, $R = \left(R_x \quad R_y\right)^T$

The elements of the reduced stiffness matrices of plate ($[A_{ij}]$, $[B_{ij}]$, etc.) are defined by

$$(A_{ij}, B_{ij}, D_{ij}, E_{ij}, F_{ij}, G_{ij}, H_{ij}) = \int_{\frac{-h_c}{2}}^{\frac{h_c}{2}} \overline{Q}_{ij}(1, z, z^2, z^3, z^4, z^5, z^6)dz \quad (i, j = 1,2,6)$$

$$(A_{ij}^x, B_{ij}^x, D_{ij}^x, E_{ij}^x, F_{ij}^x) = \int_{\frac{-h_c}{2}}^{\frac{h_c}{2}} \overline{Q}_{ij}(1, z, z^2, z^3, z^4)dz \quad (i, j = 4,5) \tag{15}$$

According to the FSDT, the elements of reduced stiffness matrices of the face sheets are defined by

- *Top face sheet*

$$(A_{ij}^t, B_{ij}^t, D_{ij}^t) = \int_{\frac{h_c}{2}}^{\frac{h_c}{2}+h_t} \overline{Q}_{ij}^{(k)}(1, z, z^2)dz = \sum_{k=1}^{n\,layer} \int_{h^k}^{h^{k+1}} \overline{Q}_{ij}^{(k)}(1, z, z^2)dz \quad (i,j=1,2,6)$$

$$(\overline{A}_{ij}^t) = \int_{\frac{h_c}{2}}^{\frac{h_c}{2}+h_t} \overline{Q}_{ij}^{(k)}\ dz = \sum_{k=1}^{n\,layer} \int_{h^k}^{h^{k+1}} \overline{Q}_{ij}^{(k)}\ dz \qquad (i,j=4,5) \tag{16}$$

• *Bottom face sheet*

$$(A_{ij}^b, B_{ij}^b, D_{ij}^b) = \int_{-\left(\frac{h_c}{2}+h_b\right)}^{-\frac{h_c}{2}} \overline{Q}_{ij}^{(k)}(1, z, z^2)dz = \sum_{k=1}^{n\,layer} \int_{h^k}^{h^{k+1}} \overline{Q}_{ij}^{(k)}(1, z, z^2)dz \quad (i,j=1,2,6)$$

$$(\overline{A}_{ij}^b) = \int_{-\left(\frac{h_c}{2}+h_b\right)}^{-\frac{h_c}{2}} \overline{Q}_{ij}^{(k)}\ dz = \sum_{k=1}^{n\,layer} \int_{h^k}^{h^{k+1}} \overline{Q}_{ij}^{(k)}\ dz \qquad (i,j=4,5) \tag{17}$$

3. New finite element formulation

The proposed finite element, named QSFT52 (Quadrilateral Sandwich First Third with 52-DOF), is a four-nodded quadrilateral sandwich plate element having thirteen DOF per node. Each node contains: two rotational DOF for each face sheet, six rotational DOF for the core, while the three translations DOF are common for sandwich layers (Fig. 3).

The displacements vectors δ at any point of coordinates (x, y) of the plate are given by

$$\delta(x, y) = \sum_{i=1}^{n} N_i(x, y)\ \delta_i \tag{18}$$

where $\delta_i = \{u_i\ v_i\ w_i\ \psi_{xi}^c\ \psi_{yi}^c\ \eta_{xi}^c\ \eta_{yi}^c\ \zeta_{xi}^c\ \zeta_{yi}^c\ \psi_{xi}^t\ \psi_{yi}^t\ \psi_{xi}^b\ \psi_{yi}^b\}^T$ is displacement vector corresponding to node i (i=1,2,3,4), and N_i are the interpolation functions (Zienkiewicz andTaylor 1977) associated with the node i (N_i=[N_1, N_2, N_3, N_4]).

The field variables may be expressed as follows

a. at mid-plate:

$$u_0(x, y) = \sum_{i=1}^{4} N_i(x, y)\ u_{0i} \quad ; \quad v_0(x, y) = \sum_{i=1}^{4} N_i(x, y)\ v_{0i} \quad ; \quad w(x, y) = \sum_{i=1}^{4} N_i(x, y)\ w_{0i} \tag{19}$$

b. core:

$$\psi_x^c(x, y) = \sum_{i=1}^{4} N_i(x, y)\psi_{xi}^c, \quad \psi_y^c(x, y) = \sum_{i=1}^{4} N_i(x, y)\psi_{yi}^c$$

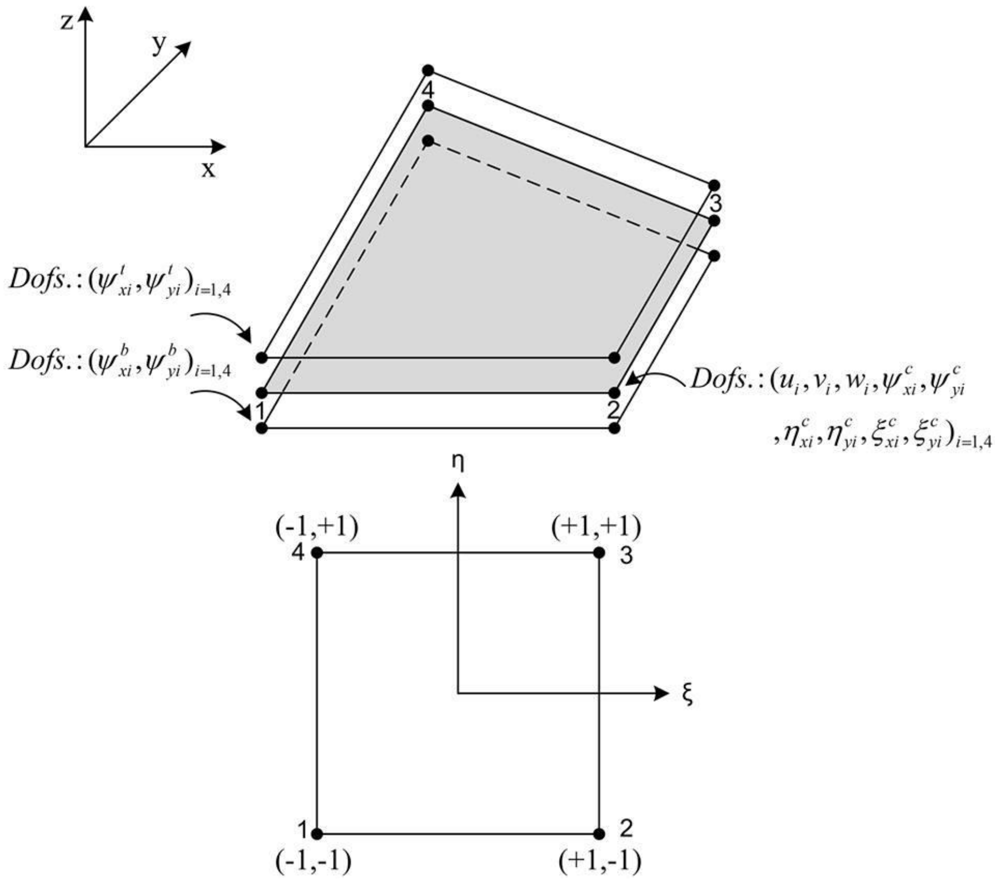

Fig. 3 Geometry and corresponding degrees of freedom of the QSFT52 element

$$\eta_x^c(x,y)=\sum_{i=1}^{4} N_i(x,y)\eta_{xi}^c, \quad \eta_y^c(x,y)=\sum_{i=1}^{4} N_i(x,y)\eta_{yi}^c$$
$$\zeta_x^c(x,y)=\sum_{i=1}^{4} N_i(x,y)\zeta_{xi}^c, \quad \zeta_y^c(x,y)=\sum_{i=1}^{4} N_i(x,y)\zeta_{yi}^c \tag{20}$$

c. top face sheet:

$$\psi_x^t(x,y)=\sum_{i=1}^{4} N_i(x,y)\psi_{xi}^t, \quad \psi_y^t(x,y)=\sum_{i=1}^{4} N_i(x,y)\psi_{yi}^t \tag{21}$$

d. bottom face sheet:

$$\psi_x^b(x,y)=\sum_{i=1}^{4} N_i(x,y)\psi_{xi}^b, \quad \psi_y^b(x,y)=\sum_{i=1}^{4} N_i(x,y)\psi_{yi}^b \tag{22}$$

For the core, the generalized strain vector (ε) of Eq. (8) at any point of coordinates (x,y) can be expressed in terms of nodal displacements as follows

$$\left\{\varepsilon^{(0)}\right\}^e = \left[B_\varepsilon^{0(c)}\right]^{(e)}\left\{\delta_i\right\}_{(e)},\ \left\{\chi^{(1)}\right\}^e = \left[B_\chi^{1(c)}\right]^{(e)}\left\{\delta_i\right\}_{(e)},\ \left\{\chi^{(2)}\right\}^e = \left[B_\chi^{2(c)}\right]^{(e)}\left\{\delta_i\right\}_{(e)}$$
$$\left\{\chi^{(3)}\right\}^e = \left[B_\chi^{3(c)}\right]^{(e)}\left\{\delta_i\right\}_{(e)},\ \left\{\gamma_s^{(0)}\right\}^e = \left[B_{\gamma_s}^{0(c)}\right]^{(e)}\left\{\delta_i\right\}_{(e)},\ \left\{\chi_s^{(1)}\right\}^e = \left[B_{\chi_s}^{1(c)}\right]^{(e)}\left\{\delta_i\right\}_{(e)} \tag{23}$$
$$\left\{\chi_s^{(2)}\right\}^e = \left[B_{\chi_s}^{2(c)}\right]^{(e)}\left\{\delta_i\right\}_{(e)}$$

where the matrices $\left[B_\varepsilon^{(0)}\right]_{3\times 52}$, $\left[B_\chi^{(1)}\right]_{3\times 52}$, $\left[B_\chi^{(2)}\right]_{3\times 52}$, $\left[B_\chi^{(3)}\right]_{3\times 52}$, $\left[B_{\gamma_s}^{(0)}\right]_{3\times 52}$, $\left[B_{\chi_s}^{(1)}\right]_{3\times 52}$ and $\left[B_{\chi_s}^{(2)}\right]_{3\times 52}$ are related the strains to nodal displacements.

For the top face sheet, the generalized strain–displacement matrices given by

$$\left\{\varepsilon_m^t\right\}^e = \left[B_m^{(t)}\right]^e\left\{\delta_i\right\}_e,\ \left\{\varepsilon_f^t\right\}^e = \left[B_f^{(t)}\right]^e\left\{\delta_i\right\}_e,\ \left\{\gamma_s^t\right\}^e = \left[B_s^{(t)}\right]^e\left\{\delta_i\right\}_e \tag{24}$$

In the same way, the generalized strain–displacement matrices for the bottom face sheet are

$$\left\{\varepsilon_m^b\right\}^e = \left[B_m^{(b)}\right]^e\left\{\delta_i\right\}_e,\ \left\{\varepsilon_f^b\right\}^e = \left[B_f^{(b)}\right]^e\left\{\delta_i\right\}_e,\ \left\{\gamma_s^b\right\}^e = \left[B_s^{(b)}\right]^e\left\{\delta_i\right\}_e \tag{25}$$

Details of $B^{(k)}$ for each layer of the sandwich plate are highlighted in Appendix A.

3.1 Introduction of assumed natural strains method

In general, a phenomenon appears in bending of thin plates known as transverse shear locking. In order to remedy this problem, Dvorkin and Bathe (1984) and Huang and Hinton (1984), have proposed the so-called ‘Assumed Natural Strains method as a solution (for more in detail see (Nayak *et al*. 2002, Lee 2004, Lee and Kim 2013, Nayak *et al*. 2003). In this work, we have used this technique at the face sheets to avoid an eventual shear locking. Therefore, assumed strains are derived by using the interpolation functions based on Lagrangian polynomial and the strain values at the sampling points where the locking does not exist (Lee and Kim 2013).

The sampling points (Lee 2004) used for natural assumed transverse shear strains of the face sheets $\gamma_{xz}^{f(A)}$ and $\gamma_{yz}^{f(A)}$ (*f=top, bottom*) are presented in Fig. 4

$$\gamma_{xz}^{f(A)} \rightarrow (0,1)_1 : (0,-1)_2, \quad \gamma_{yz}^{f(A)} \rightarrow (1,0)_1 : (-1,0)_2 \tag{26}$$

From Eq (26) the assumed natural strains are defined as follows

$$\gamma_{xz}^{f(A)} = \sum_{i=1}^{2} P_\delta(\eta)\gamma_{xz}^{\delta}, \qquad \gamma_{yz}^{f(A)} = \sum_{i=1}^{2} Q_\delta(\xi)\gamma_{yz}^{\delta} \tag{27}$$

Where δ denotes the position of the sampling point as shown in Fig. 4 and the interpolation functions P, Q are employed as follows

$$\begin{aligned} P_1 &= \frac{1}{2}(1+\eta), & P_2 &= \frac{1}{2}(1-\eta) \\ Q_1 &= \frac{1}{2}(1+\xi), & Q_2 &= \frac{1}{2}(1-\xi) \end{aligned} \tag{28}$$

The transverse shear strain-displacement relationship produced by the assumed natural strain

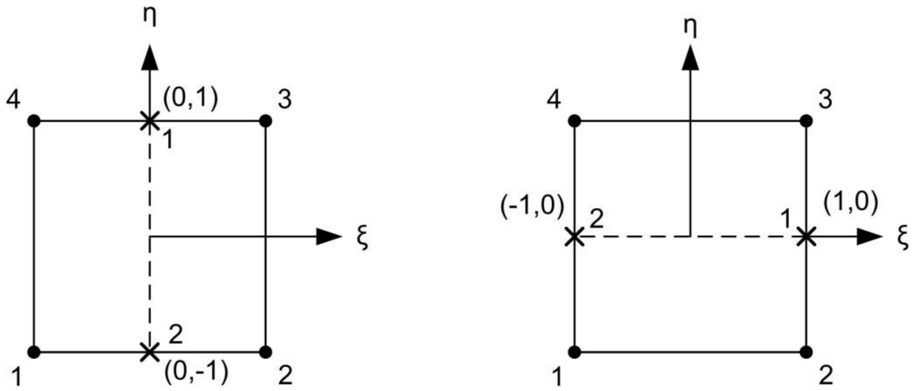

Fig. 4 The position of sampling point: (left) $\gamma_{xz}^{f(A)}$ and (right) $\gamma_{yz}^{f(A)}$

method can be written in the following matrix form

$$\begin{aligned}\left\{\overline{\gamma}_s^t\right\} &= \sum_{i=1}^{4}\left[\overline{B}_s^{t(A)}\right]\{\delta_i\} \\ \left\{\overline{\gamma}_s^b\right\} &= \sum_{i=1}^{4}\left[\overline{B}_s^{b(A)}\right]\{\delta_i\}\end{aligned} \tag{29}$$

where $\overline{B}_s^{t(A)}$ and $\overline{B}_s^{b(A)}$ are the assumed natural strain-displacement relationship matrix of top and bottom faces sheet, respectively.

3.2 Stiffness matrix calculation:

To establish the relationship between the forces and displacements, the principle of virtual work is used.

$$\delta\prod = \delta U - \delta W = 0 \tag{30}$$

Herein *U* and *W* denote the strain energy of the sandwich and the work done by the external forces respectively.

The virtual work done by a distributed transverse static load of intensity *f*(*x*,*y*)

$$\delta W = \iint f(x,y)\,\delta w\, dA \tag{31}$$

The first variation of the potential energy of the sandwich plate is the summation of contribution from the two face sheets and from the core as

$$\delta U = \int_{A_c}\int_{\frac{-h_c}{2}}^{\frac{h_c}{2}} (\sigma_{xx}^c\delta\varepsilon_{xx}^c + \sigma_{yy}^c\delta\varepsilon_{yy}^c + \sigma_{xy}^c\delta\varepsilon_{xy}^c + \sigma_{xz}^c\delta\varepsilon_{xz}^c + \sigma_{yz}^c\delta\varepsilon_{yz}^c)dV_c$$

$$+\int_{A_t}\int_{\frac{h_c}{2}}^{\frac{h_c}{2}+h_t}(\sigma_{xx}^t\delta\varepsilon_{xx}^t+\sigma_{yy}^t\delta\varepsilon_{yy}^t+\sigma_{xy}^t\delta\varepsilon_{xy}^t+\sigma_{xz}^t\delta\varepsilon_{xz}^t+\sigma_{yz}^t\delta\varepsilon_{yz}^t)dV_t$$

$$+\int_{A_b}\int_{-\left(\frac{h_c}{2}+h_b\right)}^{-\frac{h_c}{2}}(\sigma_{xx}^b\delta\varepsilon_{xx}^b+\sigma_{yy}^b\delta\varepsilon_{yy}^b+\sigma_{xy}^b\delta\varepsilon_{xy}^b+\sigma_{xz}^b\delta\varepsilon_{xz}^b+\sigma_{yz}^b\delta\varepsilon_{yz}^b)dV_b \tag{32}$$

The substitution of the expressions of the stress resultants (Eq. (14)) in the virtual work expression of the core (Eq. (32)), leads to

$$\begin{aligned}
\Pi_c=\int_A\Big(&\left\{\delta\varepsilon^{(0)}\right\}^T[A]\left\{\varepsilon^{(0)}\right\}+\left\{\delta\varepsilon^{(0)}\right\}^T[B]\left\{\chi^{(1)}\right\}+\left\{\delta\varepsilon^{(0)}\right\}^T[D]\left\{\chi^{(2)}\right\}+\left\{\delta\varepsilon^{(0)}\right\}^T[E]\left\{\chi^{(3)}\right\}\\
&+\left\{\delta\chi^{(1)}\right\}^T[B]\left\{\varepsilon^{(0)}\right\}+\left\{\delta\chi^{(1)}\right\}^T[D]\left\{\chi^{(1)}\right\}+\left\{\delta\chi^{(1)}\right\}^T[E]\left\{\chi^{(2)}\right\}+\left\{\delta\chi^{(1)}\right\}^T[F]\left\{\chi^{(3)}\right\}\\
&+\left\{\delta\chi^{(2)}\right\}^T[D]\left\{\varepsilon^{(0)}\right\}+\left\{\delta\chi^{(2)}\right\}^T[E]\left\{\chi^{(1)}\right\}+\left\{\delta\chi^{(2)}\right\}^T[F]\left\{\chi^{(2)}\right\}+\left\{\delta\chi^{(2)}\right\}^T[G]\left\{\chi^{(3)}\right\}\\
&+\left\{\delta\chi^{(3)}\right\}^T[E]\left\{\varepsilon^{(0)}\right\}+\left\{\delta\chi^{(3)}\right\}^T[F]\left\{\chi^{(1)}\right\}+\left\{\delta\chi^{(3)}\right\}^T[G]\left\{\chi^{(2)}\right\}+\left\{\delta\chi^{(3)}\right\}^T[H]\left\{\chi^{(3)}\right\}\\
&+\left\{\delta\gamma_s^{(0)}\right\}^T\left[A^s\right]\left\{\gamma_s^{(0)}\right\}+\left\{\delta\gamma_s^{(0)}\right\}^T\left[B^s\right]\left\{\chi_s^{(1)}\right\}+\left\{\delta\gamma_s^{(0)}\right\}^T\left[D^s\right]\left\{\chi_s^{(2)}\right\}\\
&+\left\{\delta\chi_s^{(1)}\right\}^T\left[B^s\right]\left\{\gamma_s^{(0)}\right\}+\left\{\delta\chi_s^{(1)}\right\}^T\left[D^s\right]\left\{\chi_s^{(1)}\right\}+\left\{\delta\chi_s^{(1)}\right\}^T\left[E^s\right]\left\{\chi_s^{(2)}\right\}\\
&+\left\{\delta\chi_s^{(2)}\right\}^T\left[D^s\right]\left\{\gamma_s^{(0)}\right\}+\left\{\delta\chi_s^{(2)}\right\}^T\left[E^s\right]\left\{\chi_s^{1}\right\}+\left\{\delta\chi_s^{(2)}\right\}^T\left[F^s\right]\left\{\chi_s^{(2)}\right\}\Big)dA-\int_A f\,\delta w dA=0
\end{aligned} \tag{33}$$

According to Eq. (23), the equilibrium equation can be expressed as follows

$$\left[K_e^{(c)}\right]\left\{d_e\right\}=\left\{f_e^{(c)}\right\} \tag{34}$$

where $\left\{f_e^{(c)}\right\}$ and $\left[K_e^{(c)}\right]$ are the load vector, the element stiffness matrix, of the core respectively. The elements stiffness matrix is computed using the Gauss numerical integration.

$$\begin{aligned}
\left[K^{(c)}\right]=\sum_e\int_{A_e}\Big(&\left[B_\varepsilon^{(0)}\right]^T[A]\left[B_\varepsilon^{(0)}\right]+\left[B_\varepsilon^{(0)}\right]^T[B]\left[B_\chi^{(1)}\right]+\left[B_\varepsilon^{(0)}\right]^T[D]\left[B_\chi^{(2)}\right]\\
&+\left[B_\varepsilon^{(0)}\right]^T[E]\left[B_\chi^{(3)}\right]+\left[B_\chi^{(1)}\right]^T[B]\left[B_\varepsilon^{(0)}\right]+\left[B_\chi^{(1)}\right]^T[D]\left[B_\chi^{(1)}\right]+\left[B_\chi^{(1)}\right]^T[E]\left[B_\chi^{(2)}\right]\\
&+\left[B_\chi^{(1)}\right]^T[F]\left[B_\chi^{(3)}\right]+\left[B_\chi^{(2)}\right]^T[D]\left[B_\varepsilon^{(0)}\right]+\left[B_\chi^{(2)}\right]^T[E]\left[B_\chi^{(1)}\right]+\left[B_\chi^{(2)}\right]^T[F]\left[B_\chi^{(2)}\right]\\
&+\left[B_\chi^{(2)}\right]^T[L]\left[B_\chi^{(3)}\right]+\left[B_\chi^{(3)}\right]^T[E]\left[B_\varepsilon^{(0)}\right]+\left[B_\chi^{(3)}\right]^T[F]\left[B_\chi^{(1)}\right]+\left[B_\chi^{(3)}\right]^T[L]\left[B_\chi^{(2)}\right]\\
&+\left[B_\chi^{(3)}\right]^T[H]\left[B_\chi^{(3)}\right]+\left[B_{\gamma_s}^{(0)}\right]^T\left[A^s\right]\left[B_{\gamma_s}^{(0)}\right]+\left[B_{\gamma_s}^{(0)}\right]^T\left[B^s\right]\left[B_{\chi_s}^{(1)}\right]+\left[B_{\gamma_s}^{(0)}\right]^T\left[D^s\right]\left[B_{\chi_s}^{(2)}\right]\\
&+\left[B_{\chi_s}^{(1)}\right]^T\left[B^s\right]\left[B_{\gamma_s}^{(0)}\right]+\left[B_{\chi_s}^{(1)}\right]^T\left[D^s\right]\left[B_{\chi_s}^{(1)}\right]+\left[B_{\chi_s}^{(1)}\right]^T\left[E^s\right]\left[B_{\chi_s}^{(2)}\right]\\
&+\left[B_{\chi_s}^{(2)}\right]^T\left[D^s\right]\left[B_{\gamma_s}^{(0)}\right]+\left[B_{\chi_s}^{(2)}\right]^T\left[E^s\right]\left[B_{\chi_s}^{(1)}\right]+\left[B_{\chi_s}^{(2)}\right]^T\left[F^s\right]\left[B_{\chi_s}^{(2)}\right]\Big)dA
\end{aligned} \tag{35}$$

Table 1 Boundary conditions used in this study

Boundary conditions	Abbreviations	Restrained edges
Simply supported	SSSS	$w_0 = \psi_x^c = \eta_x^c = \zeta_x^c = \psi_x^t = \psi_x^b = \; at\; x = \pm\frac{a}{2}$ $w_0 = \psi_y^c = \eta_y^c = \zeta_y^c = \psi_y^t = \psi_y^b = \; at\; y = \pm\frac{b}{2}$
Clamped	CCCC	$w_0 = \psi_x^c = \psi_y^c = \eta_x^c = \eta_y^c = 0$ $\zeta_x^c = \zeta_y^c = \psi_x^t = \psi_y^t = \psi_x^b = \psi_y^b = 0$

The same steps are followed to elaborate the stiffness matrix of the two face sheets, therefore:

• *Top face sheet:*

$$\left[K^{(t)}\right] = \sum_e \int_{A_e} \Big(\left[B_m^t\right]^T \left[A^{(t)}\right]\left[B_m^t\right] + \left[B_m^t\right]^T \left[B^{(t)}\right]\left[B_f^t\right] + \left[B_f^t\right]^T \left[B^{(t)}\right]\left[B_m^t\right] + \left[B_f^t\right]^T \left[D^{(t)}\right]\left[B_f^t\right] + \left[B_c^t\right]^T \left[A_c^{(t)}\right]\left[B_c^t\right] \Big) dA \tag{36}$$

• *Bottom face sheet:*

$$\left[K^{(b)}\right] = \sum_e \int_{A_e} \Big(\left[B_m^b\right]^T \left[A^{(b)}\right]\left[B_m^b\right] + \left[B_m^b\right]^T \left[B^{(b)}\right]\left[B_f^b\right] + \left[B_f^b\right]^T \left[B^{(b)}\right]\left[B_m^b\right] + \left[B_f^b\right]^T \left[D^{(b)}\right]\left[B_f^b\right] + \left[B_c^b\right]^T \left[A_c^{(b)}\right]\left[B_c^b\right] \Big) dA \tag{37}$$

Finally, the total stiffness matrix of the element is given by

$$\left[K_T\right] = \left[K^{(t)}\right] + \left[K^{(c)}\right] + \left[K^{(b)}\right] \tag{38}$$

4. Numerical results and discussions

In order to verify the performance of the developed element to convergence, stability and accuracy, different examples are studied considering symmetric/unsymmetrical composite sandwich plates with different loadings, geometry and boundary conditions. The obtained results are compared with the analytical solution given by Pagano (1970) and others finite elements numerical results found in literature.

Table 1 shows the boundary conditions, for which the numerical results have been obtained, where CCCC and SSSS respectively indicate: fully clamped and fully simply supported. The following non-dimensional quantities used in the present analysis are defined as:

Non-dimensional in-plane stresses

$$\left(\bar{\sigma}_x, \bar{\sigma}_y, \bar{\sigma}_{xy}\right) = \frac{h^2}{q_0 a^2}\left(\sigma_x, \sigma_y, \sigma_{xy}\right)$$

Non-dimensional transverse shear stresses

$$\left(\bar{\sigma}_{xz}, \bar{\sigma}_{yz}\right) = \frac{h}{q_0 a}\left(\sigma_{xz}, \sigma_{yz}\right)$$

Non-dimensional transverse displacement

$$\bar{w} = \left(\frac{100\ \mathrm{E}_2 h^3 w}{a^4 q_0}\right)$$

Example 1*. Simply supported cross-ply laminate (0/90/0) under bi-sinusoidal loading*

A simply supported three-layer square laminated plate of equal thickness, subjected to a sinusoidal loading in the two directions is considered. The mechanical characteristics of the plate are presented in Table 2. The convergence of the non-dimensional results of transverse

Table 2 Material properties for laminated plates and Sandwich

	Elastic properties						
	Location	E_1	E_2	G_{12}	G_{13}	G_{23}	$\nu_{12}=\nu_{21}$
Composite plates	All layer	25E	E	0.5E	0.5E	0.2E	0.25
Sandwich plates	Core	0.04E	0.04E	0.016E	0.06E	0.06E	0.25
	Face	25E	E	0.5E	0.5E	0.2E	0.25

Table 3 Central deflection $(\bar{w})$ at the important points of a simply supported square laminate (0/90/0) under sinusoidal load

References		Thickness ratio *h/a*		
		0.25	0.1	0.05
Present element (4×4)	QSFT52	2.0564	0.6735	0.4096
Present element (6×6)	QSFT52	2.0334	0.6921	0.4562
Present element (8×8)	QSFT52	2.0253	0.6989	0.4751
Present element (10×10)	QSFT52	2.0216	0.7021	0.4844
Present element (12×12)	QSFT52	2.0195	0.7038	0.4889
Present element (14×14)	QSFT52	2.0024	0.7049	0.4921
Present element (16×16)	QSFT52	2.0017	0.7056	0.4942
Reddy (1984)	HSDT	1.9220	0.7130	0.5041
Pagano (1970)	Elasticity solution	2.0059	0.7405	0.5164
Sheikh and Chakrabarti (2003)	HSDT	1.9230	0.7140	-
Ramesh et al. (2009)	LW	1.9927	0.7535	0.5166
Ramesh et al. (2009)	TSDT	1.9136	0.7178	0.5060
Chakrabarti and Sheikh (2004)	HOZT	1.9502	0.7522	0.5066
Kulkarni and Kapuria (2007)	RTOST	1.9248	0.7136	-
Kant and Swaminathan (2002)	HSDT	1.8948	0.7151	0.5053
Liou and Sun (1987)	Hybrid FEM	2.0200	0.7546	0.5170
Khandelwal *et al.* (2013)	HOZT	2.0151	0.7480	-

displacement with different thickness ratios (*h/a*=0.1, 0.2, and 0.25) and different mesh sizes (4×4, 6×6, 8×8, 10×10, 12×12, 14×14 and 16×16) are shown in Table 3. The obtained results are very satisfactory especially in the case of thick plates (*h/a*=0.25), where the results are in excellent agreement with the results based on 3-D elasticity solution provided by Pagano (1970) or other models in the literature (Chakrabarti and Sheikh 2004, Kant and Swaminathan 2002, Liou and Sun 1987, Ramesh *et al*. 2009, Reddy 1984, Sheikh and Chakrabarti 2003, Kulkarni and Kapuria 2007).

***Example 2**. Symmetric square sandwich plate (0/c/0) subjected to a sinusoidal load*

A simply supported square sandwich plate subjected to sinusoidal load ($q(x,y)=q_0\sin(\pi y/a)$ $\sin(\pi y/b)$) is considered. The material properties of the sandwich are presented in Table 2. The thickness of each face sheet is 0.1*h* and the thickness of the core is 0.8*h* respectively, where *h* is the total thickness of the plate. The non-dimensional results of transverse displacement, in plane normal stresses and transverse shear stress for different mesh sizes and thickness ratios are displayed on Table 4. Distributions of non-dimensional in-plane stresses through the thickness are plotted with the 3D elasticity solution given by Pagano (1970) in Figs. 5 and 6 for *h/a* ratio equal to 0.25 and 0.1. It was found that the present results especially for the transverse shear stresses, are in excellent agreement with those obtained by the elasticity solution given by Pagano (1970) and other finite elements models based on different theories (Chalak *et al*. 2012, Kant and Kommineni 1992, Kant and Swaminathan 2002, Khandelwal *et al*. 2013, Nayak *et al*. 2003, Tu *et al*. 2010, Wu and Lin 1993, Pandit *et al*. 2008, Ramtekkar *et al*. 2003, Singh *et al*. 2011), which shows the performances and convergence of the proposed formulation.

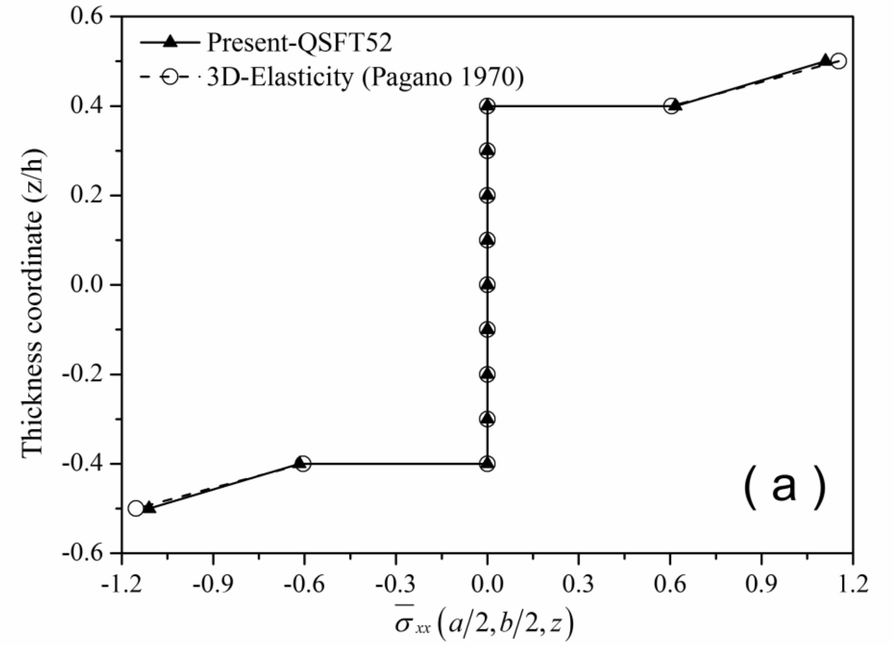

Fig. 5 Variation of non-dimensional (a) in-plane stress ($\bar{\sigma}_{xx}$) and (b) in-plane stress ($\bar{\sigma}_{yy}$), through the thickness of simply suported square sandwich plate under sinusoidal transverse load (*a/h*=10)

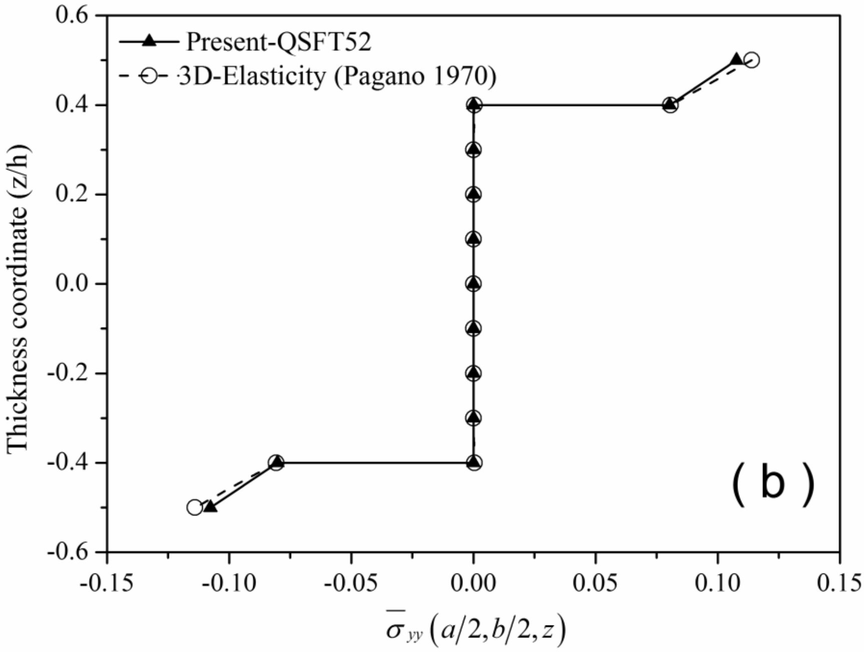

Fig. 5 Continued

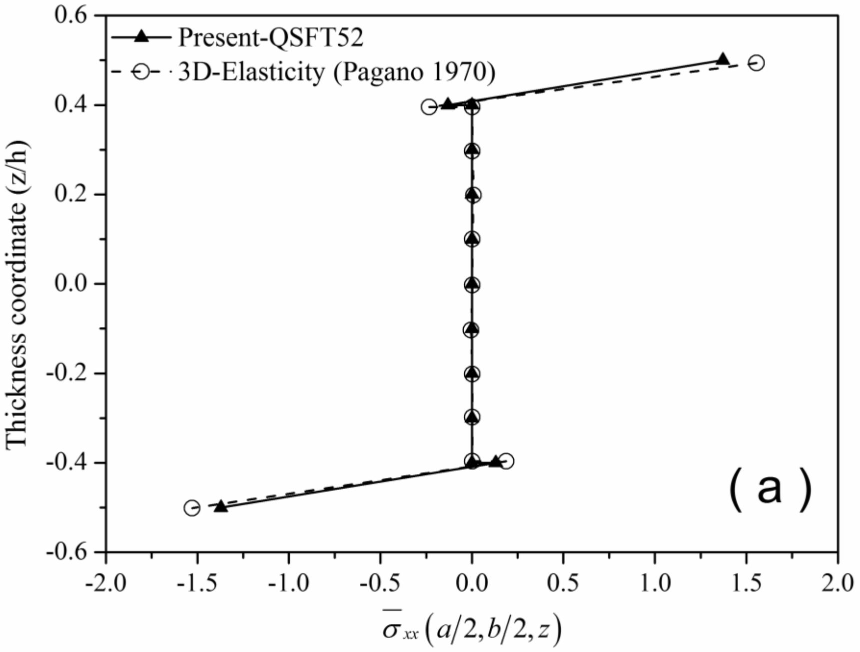

Fig. 6 Variation of non-dimensional (a) in-plane stress ($\bar{\sigma}_{xx}$), (b) in-plane stress ($\bar{\sigma}_{yy}$) and (c) in-plane shear stress ($\bar{\sigma}_{xy}$), through the thickness of simply suported square sandwich plate under sinusoidal transverse load (*a/h*=4)

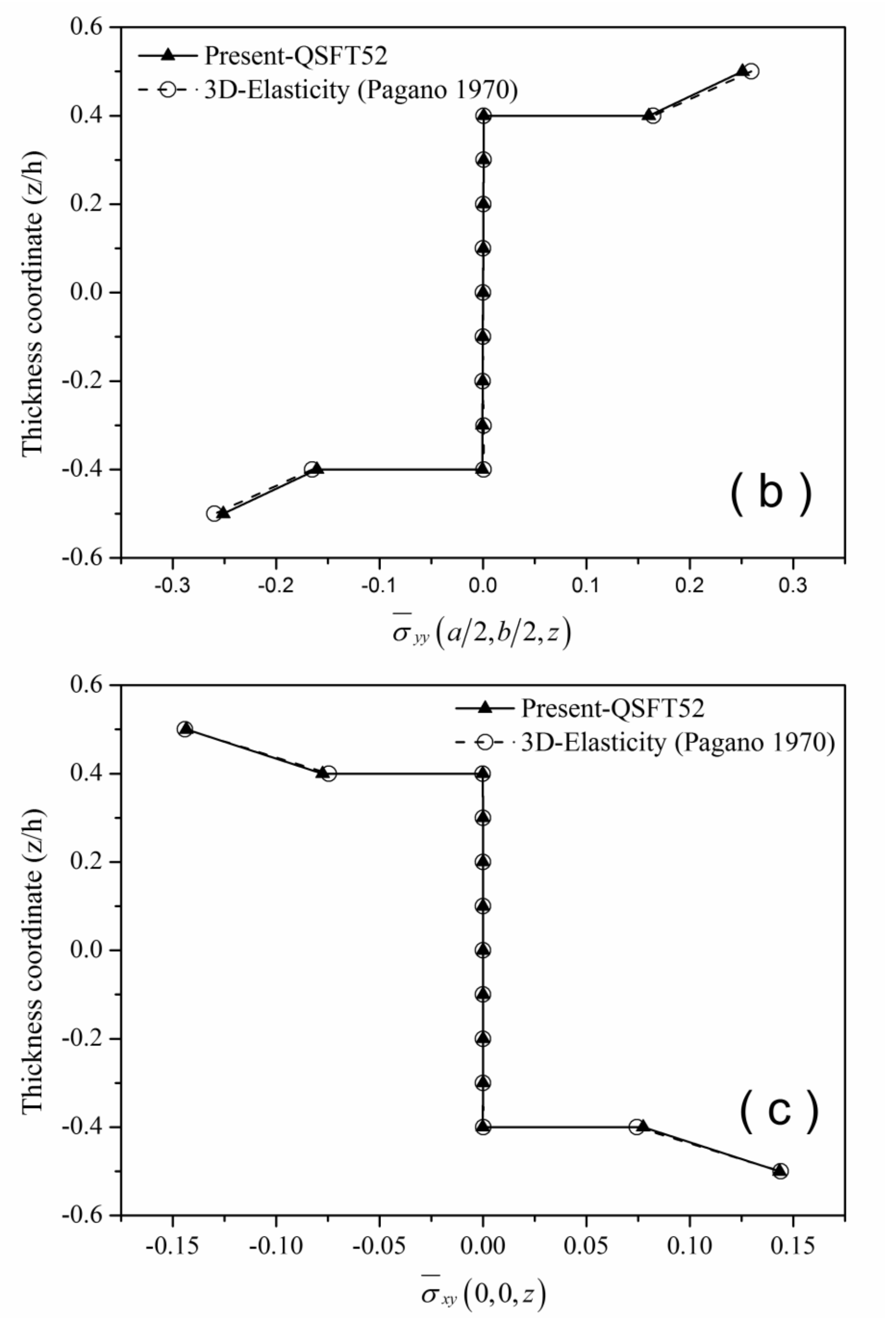

Fig. 6 Continued

***Example 3**. Symmetric square sandwich plate (0/c/0) subjected to uniformly distributed load*

This example has been studied by Khatua and Cheung (1973), Topdar *et al*. (2003) and Chakrabarti and Sheikh (2004). The sandwich plate is defined by the dimensions (a=b=254 mm) and a thickness h=20.4724 mm. Each face sheet has a thickness of 0.7112 mm. In the first case, the plate is fully simply supported (SSSS) and subjected to a uniformly distributed load F=0.00688 N/mm^2.

The material properties are:

Face layers: $E_{11}=E_{22}$=68.8 GPa, $G_{13}=G_{23}$=27.52 GPa and v_{13}=0.3

Core: $E_{11}=E_{22}=6.88\times10^{-12}$ GPa, $G_{13}=G_{23}$=0.2064 GPa and v_{13}=0.3

In the second case, the plate is fully clamped (CCCC). The mechanical properties are the same as in case one, except for the transverse shear rigidity of the core $G_{13}=G_{23}$=0.3131 GPa. The results of the transverse displacement, in-plane normal stress and transverse shear stress with different mesh sizes of (8×8, 12×12 and 16×16) are reported in Table 5. The results obtained by the present element are in excellent agreement with those obtained by the analytical solution given by Azar (1968) and the numerical results given by (Chakrabarti and Sheikh 2004, Khatua and Cheung 1973, Topdar *et al*. 2003).

Example 4*. All edges clamped square sandwich plate (0/c/0) under uniformly distributed load*

In this test, the same geometrical and mechanical properties as in example 2 have been adopted. The plates are fully clamped (CCCC) and subjected to a uniformly distributed load. The non-dimensional results of transverse displacement, in-plane normal stresses at the top and the bottom faces sheets and the transverse shear stress at the important points for different thickness ratios (h/a=0.01, 0.02, 0.05, 0.1 and 0.25) are presented in Table 6 using mesh size of (16×16). The variation of the non-dimensional deflection $(\bar{w})$ with different thickness ratios has been plotted as shown in Fig. 7. It was seen that the values of non-dimensional transverse displacement $(\bar{w})$

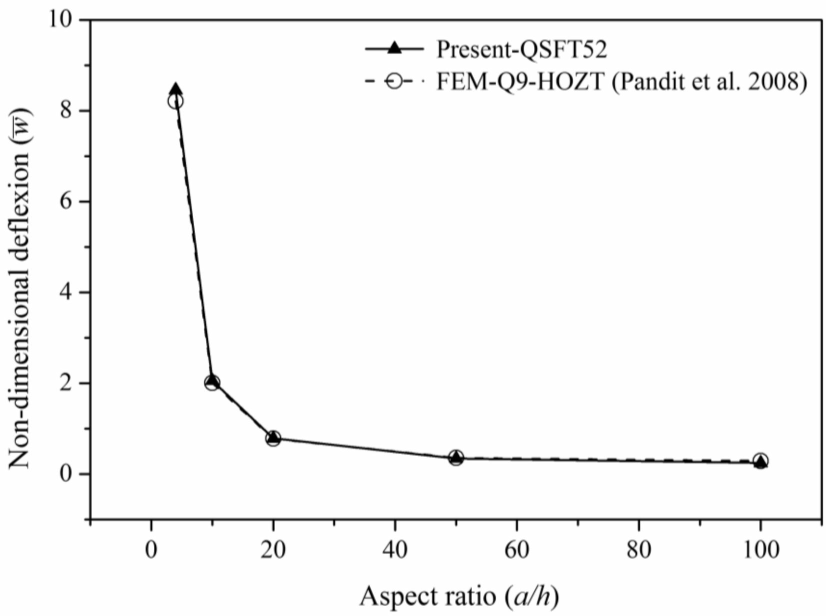

Fig. 7 Effect of aspect ratio (a/h) on the non-dimensional transverse displacement $(\bar{w})$ of square clamped sandwich plates (0/c/0) under sinusoidal loading

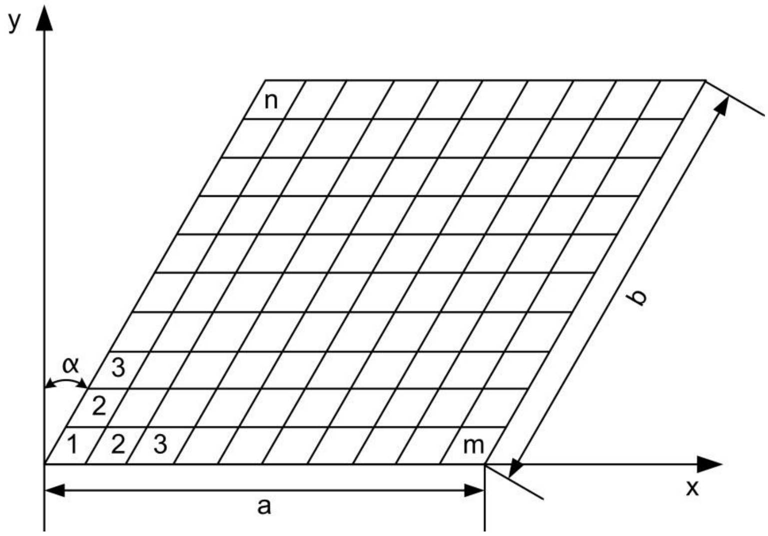

Fig. 8 A skew plate with mesh arrangement (mesh size: $m \times n$)

decreases when increasing (*h/a*) ratio. This is due to the effect of the thickness of the core (0.8*h*) which has an important role in the sandwich plates because; it considerably affects the flexural rigidity. The numerical results of the present element are very close with the finite element results obtained by Pandit *et al*. (2008) using a nine-nodded isoparametric element with eleven degrees of freedom (11 DOF) per node, based on a higher order Zig-Zag theory. It can be noticed that the present model is applicable in both thick and thin sandwich plates.

***Example 5**. Square sandwich plate* ($\theta/\ \theta$+90/*C*/ $\theta/\ \theta$+90) *with an angle-ply laminated stiff sheets at the two faces subjected to uniformly distributed load*

This example has been chosen to test the performance of our element (QSFT52) in sandwich plates with laminated face sheets. A square sandwich plates with an angle-ply laminated stiff sheets ($\theta/\ \theta$+90/*C*/ $\theta/\ \theta$+90) at the two faces and subjected to a uniformly distributed load is considered. The thickness of each laminate layer is $0.05h$, whereas the thickness of the core is $0.8h$. The mechanical properties of materials used are listed in Table 2. The non-dimensional results of transverse displacement, in-plane stresses and transverse shear stresses obtained in the present analysis for three orientation angles on the face sheets (0°, 30° and 45°) and three thickness ratios (*h/a*=0.05, 0.1 and 0.2) are presented in Table 7. The obtained results (for a mesh size of 12×12) are compared with those obtained by Chakrabarti and Sheikh (2005) and Khandelwal *et al*. (2013). The obtained results present a good performance and also confirm the robustness of the QSFT52 element.

***Example 6**. Simply supported cross-ply (0/90/0) skew laminated plate under uniformly distributed load*

In the present study, a three-layered skew laminated plate (Fig. 8) of equal thickness, subjected to uniformly distributed load is considered. The mechanical characteristics of the plate are listed in Table 2. In this example, three skew angles (30°, 45° and 60°) with two thickness ratios (*h/a*=0.1 and 0.2) have been considered. The results of the normalized transverse displacement at the center

Table 4 Normalized maximum deflection $(\bar{w})$ and stresses $(\bar{\sigma}_{xx}, \bar{\sigma}_{yy}, \bar{\sigma}_{xy}, \bar{\sigma}_{xz}, \bar{\sigma}_{yz})$ at the important points of a simple supported simply supported square sandwich plate (0/c/0) under sinusoidal loading

h/a	Reference		$\bar{w}$ (*a*/2, *b*/2,0)	$\bar{\sigma}_{xx}$ (*a*/2, *b*/2, *h*/2)	$\bar{\sigma}_{yy}$ (*a*/2, *b*/2, *h*/2)	$\bar{\sigma}_{xz}$ (0, *b*/2, 0)	$\bar{\sigma}_{yz}$ (*a*/2, 0, 0)	$\bar{\sigma}_{xy}$ (0, 0, *h*/2)
0.5	Present element (8×8)	QSFT52	23.4200	2.2463	0.3931	0.1766	0.1363	0.2283
	Present element (10×10)	QSFT52	23.3493	2.2886	0.4014	0.1803	0.1388	0.2330
	Present element (12×12)	QSFT52	23.3106	2.3119	0.4060	0.1823	0.1401	0.2356
	Present element (14×14)	QSFT52	23.2875	2.3260	0.4088	0.1835	0.1409	0.2372
	Present element (16×16)	QSFT52	23.2725	2.3351	0.4106	0.1843	0.1414	0.2382
	Pagano (1970)	Elasticity	21.6531	2.6530	0.3920	0.1850	0.1400	0.2340
	Ramtekkar *et al*. (2003)	LWT (FE-3D)	-	2.6840	0.3960	0.1860	0.1420	0.2360
	Kant and Kommineni (1992)	TSDT	21.3707	2.7985	-	-	-	0.2371
0.25	Present element (8×8)	QSFT52	7.7651	1.3281	0.2399	0.2255	0.1038	0.1386
	Present element (10×10)	QSFT52	7.7526	1.3563	0.2452	0.2303	0.1052	0.1417
	Present element (12×12)	QSFT52	7.7457	1.3719	0.2481	0.2330	0.1059	0.1434
	Present element (14×14)	QSFT52	7.7416	1.3813	0.2499	0.2346	0.1064	0.1444
	Present element (16×16)	QSFT52	7.7388	1.3875	0.2511	0.2357	0.1067	0.1451
	Pagano (1970)	Elasticity	7.5962	1.5160	0.2595	0.2390	0.1072	0.1440
	Pandit *et al*. (2008)	HOZT	7.6552	1.5218	0.2506	0.2520	0.1156	0.1468
	Tu *et al*. (2010)	TSDT	7.5610	1.5518	0.2483	0.2447	0.1184	0.1459
	Singh *et al*. (2011)	HOZT	7.8556	1.5480	-	0.2611	-	0.1671
	Khandelwal *et al*. (2013)	HOZT	7.5873	1.5316	0.2674	0.2538	0.1192	-
	Chalak *et al*. (2012)	HOZT	7.5822	1.5306	0.2581	0.2436	0.1147	0.1445
	Ramtekkar *et al*. (2003)	LWT (FE-3D)	-	1.5700	0.2600	0.2400	0.1080	0.1450
	Wu and Lin (1993)	LWT	-	1.5480	0.2413	0.2497	-	0.1339
	Pandya and Kant (1988)	HSDT	0.6947	1.5230	0.2414	0.2750	-	0.1419
	Manjunatha and Kant (1993)	HOST	7.1596	-	-	0.2370	0.1040	-
	Kant and Kommineni (1992)	TSDT	7.1502	1.4989	-	-	-	0.1428
	Kant and Swaminathan (2002)	HSDT	7.0551	1.5137	0.2648	-	-	0.1379

Table 4 Continued

h/a	Reference		$\overline{w}$ $(a/2, b/2, 0)$	$\overline{\sigma}_{xx}$ $(a/2, b/2, h/2)$	$\overline{\sigma}_{yy}$ $(a/2, b/2, h/2)$	$\overline{\sigma}_{xz}$ $(0, b/2, 0)$	$\overline{\sigma}_{yz}$ $(a/2, 0, 0)$	$\overline{\sigma}_{xy}$ $(0, 0, h/2)$
0.2	Present element (8×8)	QSFT52	5.5650	1.2038	0.1972	0.2424	0.0893	0.1157
	Present element (10×10)	QSFT52	5.5600	1.2311	0.2017	0.2476	0.0903	0.1183
	Present element (12×12)	QSFT52	5.5571	1.2461	0.2042	0.2505	0.0908	0.1197
	Present element (14×14)	QSFT52	5.5554	1.2552	0.2057	0.2523	0.0911	0.1206
	Present element (16×16)	QSFT52	5.5554	1.2612	0.2067	0.2535	0.0913	0.1212
	Pagano (1970)	Elasticity	5.4746	1.3704	0.2094	0.2569	0.0918	-
	Khandelwal *et al*. (2013)	HOZT	5.4464	1.3617	0.2216	0.2530	0.1025	-
0.1	Present element (8×8)	QSFT52	2.1964	1.0484	0.1020	0.2815	0.0538	0.0662
	Present (10×10)	QSFT52	2.2036	1.0777	0.1047	0.2880	0.0534	0.0680
	Present element (12×12)	QSFT52	2.2075	1.0939	0.1062	0.2916	0.0532	0.0690
	Present element (14×14)	QSFT52	2.2099	1.1038	0.1071	0.2938	0.0531	0.0696
	Present element (16×16)	QSFT52	2.2115	1.1103	0.1077	0.2952	0.0530	0.0699
	Pagano (1970)	Elasticity	2.2004	1.1531	0.1104	0.3000	0.0530	0.0707
	Pandit *et al*. (2008)	HOZT	2.2002	1.1483	0.1086	0.3158	0.0570	0.0709
	Tu *et al*. (2010)	TSDT	2.2027	1.1466	0.1105	0.3181	0.0532	0.0715
	Singh *et al*. (2011)	HOZT	2.2389	1.1594	-	0.3237	-	0.0759
	Khandelwal *et al*. (2013)	HOZT	2.1786	1.1539	0.1184	0.3185	0.0598	-
	Chalak *et al*. (2012)	HOZT	2.1775	1.1528	0.1143	0.3058	0.0575	0.0705
	Ramtekkar *et al.* (2003)	LWT (FE-3D)	-	1.1590	0.1110	0.3030	0.0550	0.0720
	Wu and Lin (1993)	LWT	-	1.2100	0.1115	0.3240	-	0.0713
	Pandya and Kant (1988)	HSDT	0.2023	1.1660	0.1052	0.3400	-	0.0692
	Kant and Kommineni (1992)	TSDT	2.0864	1.1657	-	-	-	0.0692
	Kant and Swaminathan (2002)	HSDT	2.0798	1.1523	0.1100	-	-	0.0685
	Nayak *et al*. (2003)	HSDT (Q4)	-	1.1410	0.1034	0.3465	0.0574	0.0685
	Nayak *et al*. (2003)	HSDT (Q9)	-	1.1510	0.1043	0.3506	0.0580	0.0689

Table 4 Continued

h/a	Reference		$\overline{w}$ $(a/2, b/2, 0)$	$\overline{\sigma}_{xx}$ $(a/2, b/2, h/2)$	$\overline{\sigma}_{yy}$ $(a/2, b/2, h/2)$	$\overline{\sigma}_{xz}$ $(0, b/2, 0)$	$\overline{\sigma}_{yz}$ $(a/2, 0, 0)$	$\overline{\sigma}_{xy}$ $(0, 0, h/2)$
0.05	Present element (8×8)	QSFT52	1.1766	0.9895	0.0627	0.2944	0.0430	0.0459
	Present element (10×10)	QSFT52	1.1953	1.0292	0.0652	0.3025	0.0407	0.0477
	Present element (12×12)	QSFT52	1.2058	1.0516	0.0666	0.3069	0.0393	0.0487
	Present element (14×14)	QSFT52	1.2122	1.0653	0.0674	0.3097	0.0385	0.0493
	Present element (16×16)	QSFT52	1.2164	1.0743	0.0680	0.3115	0.0379	0.0497
	Pagano (1970)	Elasticity	1.2264	1.1100	0.0700	0.3174	0.0361	0.0511
	Pandit *et al*. (2008)	HOZT	1.2254	1.1055	0.0694	0.3342	0.0392	0.0509
	Singh *et al*. (2011)	HOZT	1.2424	1.1161	-	0.3429	-	0.0536
	Khandelwal *et al*. (2013)	HOZT	1.2128	1.1113	0.0769	0.3374	0.0415	-
	Chalak *et al.* (2012)	HOZT	1.2121	1.1103	0.0742	0.3272	0.0399	0.0508
	Ramtekkar *et al*. (2003)	LWT (FE-3D)	-	1.1150	0.0700	0.3170	0.0360	0.0510
	Wu and Lin (1993)	LWT	-	1.1730	0.0724	0.3530	-	0.0525
	Kant and Kommineni (1992)	TSDT	1.1947	1.1246	-	-	-	0.0506
	Kant and Swaminathan (2002)	HSDT	1.1933	1.1110	0.0705	-	-	0.0504
0.02	Present element (8×8)	QSFT52	0.7347	0.8099	0.0419	0.2801	0.0646	0.0329
	Present element (10×10)	QSFT52	0.7962	0.8979	0.0465	0.2937	0.0547	0.0365
	Present element (12×12)	QSFT52	0.8341	0.9523	0.0493	0.3019	0.0483	0.0387
	Present element (14×14)	QSFT52	0.8588	0.9877	0.0511	0.3072	0.0441	0.0401
	Present element (16×16)	QSFT52	0.8756	1.0119	0.0524	0.3107	0.0412	0.0411
	Pagano (1970)	Elasticity	0.9348	1.0990	0.0569	0.3230	0.0306	0.0446
	Pandit *et al*. (2008)	HOZT	0.9341	1.0948	0.0566	0.3403	0.0333	0.0445
	Singh *et al*. (2011)	HOZT	0.9458	1.1050	-	0.3617	-	0.0465
	Chalak *et al*. (2012)	HOZT	0.9248	1.0997	0.0611	0.3300	0.0321	0.0443

Table 5 Central deflection $(\bar{w})$ and stresses (σ_{xx}, σ_{yy}, σ_{xz}, σ_{yz}, σ_{xy}) at the important points of a simple supported square sandwich plate under uniformly distributed load

h/a	Reference		w100 (mm)	$\sigma_{xx}(a/2, b/2, h/2)$	$\sigma_{yy}(a/2, b/2, h/2)$	$\sigma_{xx}(0, b/2, 0)$	$\sigma_{yz}(a/2, 0, 0)$	$\sigma_{xy}(0, 0, h/2)$
Cas I	Present element (8×8)	QSFT52	1.8679	1.5146	1.5146	0.0244	0.0244	-0.9700
	Present element (12×12)	QSFT52	1.8745	1.5588	1.5588	0.0262	0.0262	-1.0396
	Present element (16×16)	QSFT52	1.8767	1.5742	1.5742	0.0270	0.0270	-1.0704
	Khatua and Cheung (1973)	-	1.8697	-	-	-	-	-
	Azar (1968)	Analytical	1.8780	-	-	-	-	-
	Chakrabarti and Sheikh (2004)	RHSDT	1.8750	1.5817	1.5817	0.0284	-	-
	Chakrabarti and Sheikh (2004)	RFSDT	1.8682	1.5816	1.5816	0.0297	-	-
	Topdar *et al*. (2003)	PRHSDT	1.8793	-	-	0.0232	0.0232	-
Cas II	Present element (8×8)	QSFT52	0.8813	0.7906	0.7906	0.0221	0.0221	-0.1802
	Present element (12×12)	QSFT52	0.8750	0.8149	0.8149	0.0246	0.0246	-0.1762
	Present element (16×16)	QSFT52	0.8717	0.8141	0.8141	0.0252	0.0252	-0.1664
	Khatua and Cheung (1973)	-	0.8707	-	-	-	-	-
	Chakrabarti and Sheikh (2004)	RHSDT	0.9535	0.8916	0.8916	0.0558	-	-
	Chakrabarti and Sheikh (2004)	RFSDT	0.8880	0.8225	0.8225	0.0475	-	-
	Folie (1970)	-	0.8814	-	-	-	-	-

Table 6 Normalized maximum deflection $(\overline{w})$ and stresses $(\overline{\sigma}_{xx}, \overline{\sigma}_{yy}, \overline{\sigma}_{xy}, \overline{\sigma}_{xz}, \overline{\sigma}_{yz})$ at the important points of a clamped square sandwich plate (0/*c*/0) under uniformly distributed load

h/a	Reference		$\overline{w}$ (*a*/2, *b*/2, ±*h*/2)	$\overline{\sigma}_{xx}$ (*a*/2, *b*/2, ±*h*/2)	$\overline{\sigma}_{yy}$ (*a*/2, *b*/2, ±*h*/2)	$\overline{\sigma}_{xz}$ (0, *b*/2, 0)	$\overline{\sigma}_{yz}$ (*a*/2, 0, 0)	$\overline{\sigma}_{xy}$ (0, 0, ±*h*/2)
0.01	Present element	QSFT52	0.2458 0.2458	0.4490 -0.4490	0.0178 -0.0178	0.5120	0.2321	-0.0018 0.0018
	Pandit *et al*. (2008)	HOZT	0.2897 0.2897	0.5398 -0.5398	0.0099 -0.0099	0.5429	0.1764	-0.0025 0.0025
0.02	Present element	QSFT52	0.3458 0.3458	0.5226 -0.5226	0.0189 -0.0189	0.5024	0.1841	-0.0037 0.0037
	Pandit *et al*. (2008)	HOZT	0.3549 0.3549	0.5478 -0.5478	0.0131 -0.0131	0.5138	0.1806	-0.0040 0.0040
0.05	Present element	QSFT52	0.7871 0.7871	0.5576 -0.5576	0.0402 -0.0402	0.4528	0.1776	-0.0098 0.0098
	Pandit *et al*. (2008)	HOZT	0.7793 0.7789	0.5754 -0.5754	0.0371 -0.0371	0.4368	0.2020	-0.0089 0.0089
0.1	Present element	QSFT52	2.0585 2.0585	0.6011 -0.6011	0.0999 -0.0999	0.3761	0.2049	- 0.0197 0.0197
	Pandit *et al*. (2008)	HOZT	2.0090 2.0022	0.6346 -0.6346	0.0951 -0.0952	0.3367	0.2372	- 0.0171 0.0163
0.25	Present element	QSFT52	8.4575 8.4575	1.0148 -1.0148	0.2070 -0.2070	0.2751	0.2212	-0.0457 0.0457
	Pandit *et al*. (2008)	HOZT	8.2090 7.9482	1.1809 -1.1819	0.1919 -0.1923	0.2242	0.2630	-0.0401 0.0314

Table 7 Normalized maximum deflection $(\bar{w})$ and stresses $(\bar{\sigma}_{xx}, \bar{\sigma}_{yy}, \bar{\sigma}_{xy}, \bar{\sigma}_{xz}, \bar{\sigma}_{yz})$ at the important points of a simple supported simply supported square sandwich plate with angle-ply laminated faces (*θ*/ *θ*+90/*C*/ *θ*/ *θ*+90) under uniformly distributed load

h/*a*	Reference		$\bar{w}$ (*a*/2, *b*/2, 0)	$\bar{\sigma}_{xx}$ (*a*/2, *b*/2, *h*/2)	$\bar{\sigma}_{yy}$ (*a*/2, *b*/2, *h*/2)	$\bar{\sigma}_{xz}$ (0, *b*/2, ±0.4*h*)	$\bar{\sigma}_{yz}$ (*a*/2, 0, ±0.4*h*)
$\theta = 0°$ 0.05	Present element	QSFT52	1.6766	1.6197	1.6197	0.3408	0.3408
	Pagano (1970)	Elasticity	1.6957	1.5851	1.5692	0.3560	0.3563
	Khandelwal *et al*. (2013)	HOZT	1.7107	1.6265	1.5653	0.4515	0.5230
	Chakrabarti and Sheikh (2005)	HOZT	1.7126	1.5988	-	0.3732	-
0.1	Present element	QSFT52	2.6149	1.7320	1.7320	0.3337	0.3337
	Pagano (1970)	Elasticity	2.6168	1.6004	1.5794	0.3496	0.3503
	Khandelwal *et al*. (2013)	HOZT	2.6295	1.6537	1.5829	0.4142	0.4142
	Chakrabarti and Sheikh (2005)	HOZT	2.6296	1.6249	-	0.3612	-
0.2	Present element	QSFT52	6.2940	2.1538	2.1538	0.3242	0.3242
	Pagano (1970)	Elasticity	6.2981	1.7093	1.7523	0.3436	0.3413
	Khandelwal *et al*. (2013)	HOZT	6.3001	1.8111	1.7328	0.3982	0.3993
	Chakrabarti and Sheikh (2005)	HOZT	6.3016	1.7792	-	0.3482	-
$\theta = 30°$ 0.05	Present element	QSFT52	1.2199	0.7884	0.7884	0.3465	0.3465
	Khandelwal *et al*. (2013)	HOZT	1.2450	0.7985	0.7666	0.4637	0.5079
	Chakrabarti and Sheikh (2005)	HOZT	1.2381	0.7653	-	0.3603	-
0.1	Present element	QSFT52	2.2137	0.9575	0.9575	0.3406	0.3406
	Khandelwal *et al*. (2013)	HOZT	2.2322	0.9290	0.8840	0.4280	0.4409
	Chakrabarti and Sheikh (2005)	HOZT	2.2237	0.8882	-	0.3659	-
0.2	Present element	QSFT52	5.9326	2.1538	2.1538	0.3382	0.3382
	Khandelwal *et al*. (2013)	HOZT	5.9579	1.1733	1.1074	0.4376	0.4321
	Chakrabarti and Sheikh (2005)	HOZT	5.9463	1.1165	-	0.3762	-
$\theta = 45°$ 0.05	Present element	QSFT52	1.0671	0.4366	0.4366	0.3215	0.3215
	Khandelwal *et al*. (2013)	HOZT	1.0773	0.4479	0.4228	0.4621	0.5309
	Chakrabarti and Sheikh (2005)	HOZT	1.0615	0.4247	-	0.2197	-
0.1	Present element	QSFT52	2.0035	0.4991	0.4991	0.3223	0.3223
	Khandelwal *et al*. (2013)	HOZT	1.9950	0.4698	0.4422	0.4445	0.4592
	Chakrabarti and Sheikh (2005)	HOZT	1.9764	0.4444	-	0.2203	-
0.2	Present element	QSFT52	5.6615	0.7022	0.7022	0.3144	0.3144
	Khandelwal *et al*. (2013)	HOZT	5.6329	0.5755	0.5408	0.4612	0.4484
	Chakrabarti and Sheikh (2005)	HOZT	5.6079	0.5516	-	0.2197	-

Table 8 Normalized maximum deflection ($\bar{w}$) of a simple supported simply supported cross-ply (0/90/0) skew laminate plate under uniformly distributed load

h/a	Skew angle	Reference		$\bar{w}$ (a/2, b/2,0)
0.1	30°	Present element	QSFT52	0.8452
		Chakrabarti and Sheikh (2004)	RHSDT	0.8814
		Chakrabarti and Sheikh (2004)	FSDT	0.9182
		Sheikh and Chakrabarti (2003)	HSDT	0.8621
		Ramesh *et al*. (2009)	LWT	0.9013
		Ramesh *et al*. (2009)	TSDT	0.8666
		Kulkarni and Kapuria (2007)	RTSDT	0.8666
		Chalak *et al*. (2014)	HOZT	0.8366
	45°	Present element	QSFT52	0.5758
		Chakrabarti and Sheikh (2004)	RHSDT	0.5742
		Chakrabarti and Sheikh (2004)	FSDT	0.6045
		Ramesh *et al*. (2009)	LWT	0.5939
		Ramesh *et al*. (2009)	TSDT	0.5745
		Sheikh and Chakrabarti (2003)	HSDT	0.5707
		Kulkarni and Kapuria (2007)	RTSDT	0.5725
		Chalak *et al*. (2014)	HOZT	0.5611
	60°	Present element	QSFT52	0.2599
		Chakrabarti and Sheikh (2004)	RHSDT	0.2481
		Chakrabarti and Sheikh (2004)	FSDT	0.2642
		Ramesh *et al*. (2009)	LWT	0.2602
		Ramesh *et al*. (2009)	TSDT	0.2541
		Sheikh and Chakrabarti (2003)	HSDT	0.2505
		Kulkarni and Kapuria (2007)	RTSDT	0.2461
		Chalak *et al*. (2014)	HOZT	0.2490
		Kabir (1995)	FSDT	0.2600
0.2	30°	Present element	QSFT52	1.8328
		Chakrabarti and Sheikh (2004)	RHSDT	1.6811
		Chakrabarti and Sheikh (2004)	FSDT	1.8642
		Ramesh *et al*. (2009)	LWT	1.7350
		Ramesh *et al*. (2009)	TSDT	1.6713
		Chalak *et al*. (2014)	HOZT	1.6904
	45°	Present element	QSFT52	1.3089
		Chakrabarti and Sheikh (2004)	RHSDT	1.1790
		Chakrabarti and Sheikh (2004)	FSDT	1.2174
		Ramesh *et al*. (2009)	LWT	1.1248
		Ramesh *et al*. (2009)	TSDT	1.0980
		Chalak *et al*. (2014)	HOZT	1.1496
	60°	Present element	QSFT52	0.6208
		Chakrabarti and Sheikh (2004)	RHSDT	0.5196
		Chakrabarti and Sheikh (2004)	FSDT	0.5158
		Ramesh *et al*. (2009)	LWT	0.5210
		Ramesh *et al*. (2009)	TSDT	0.5185
		Chalak *et al*. (2014)	HOZT	0.5073

of the plate are presented in Table 8 using mesh size of (12×12). It may be observed that the results of developed element are very close with the results reported by Chakrabarti and Sheikh (2004), Sheikh and Chakrabarti (2003), Kabir (1995), Ramesh *et al*. (2009), Chalak *et al*. (2014), Kulkarni and Kapuria (2007).

5. Conclusions

This paper reports the results of a new layerwise isoparametric finite element model for bending analysis of sandwich plates. The model is based on the third order shear deformation theory for the core and the first order shear deformation theory for the face sheets. The proposed finite element is a four-nodded quadrilateral isoparametric sandwich plate element (QSFT52) having thirteen degrees of freedom per node (13 DOF). The so-called 'Assumed Natural Strains method' was used to avoid an eventual locking phenomenon. The displacement continuity condition at the interfaces 'face sheets-core' is satisfied.

The performance of the developed element was tested by different examples for symmetric/ unsymmetric composite laminated, sandwich and skew plates with different aspect ratios, loadings and boundary conditions. The obtained numerical results were compared with those obtained by the analytical solutions and other finite element models found in literature.

The use of the proposed finite element and the combination of the first order shear deformation theory and the third-order plate theory, used respectively to modulate the face sheets and the core of sandwich, showed a good accuracy and convergence speed for both thin and thick plates.

References

Aydogdu, M. (2009), "A new shear deformation theory for laminated composite plates", *Compos. Struct.*, **89**(1), 94-101.

Azar, J.J. (1968), "Bending theory for multilayer orthotropic sandwich plates", *AIAA J.*, **6**(11), 2166-2169.

Carrera, E. (2002), "Theories and finite elements for multilayered, anisotropic, composite plates and shells", *Arch. Comput. Meth. Eng.*, **9**(2), 87-140.

Carrera, E. (2003), "Historical review of zig-zag theories for multilayered plates and shells", *Appl. Mech. Rev.*, **56**, 287-308.

Ćetković, M. and Vuksanović, D. (2009), "Bending, free vibrations and buckling of laminated composite and sandwich plates using a layerwise displacement model", *Compos. Struct.*, **88**(2), 219-227.

Chakrabarti, A. and Sheikh, A.H. (2004), "A new triangular element to model inter-laminar shear stress continuous plate theory", *Int. J. Numer. Meth. Eng.*, **60**(7), 1237-1257.

Chakrabarti, A. and Sheikh, A.H. (2005), "Analysis of laminated sandwich plates based on interlaminar shear stress continuous plate theory", *J. Eng. Mech.*, **131**(4), 377-384.

Chalak, H.D., Chakrabarti, A., Iqbal, M.A. and Sheikh, A.H. (2012), "An improved C0 FE model for the analysis of laminated sandwich plate with soft core", *Finite Elem. Anal. Des.*, **56**, 20-31.

Chalak, H.D., Chakrabarti, A., Sheikh, A.H. and Iqbal, M.A. (2014), "C0 FE model based on HOZT for the analysis of laminated soft core skew sandwich plates: Bending and vibration", *Appl. Math. Model.*, **38**(4), 1211-1223.

Cho, M. and Parmerter, R. (1993), "Efficient higher order composite plate theory for general lamination configurations", *AIAA J.*, **31**(7), 1299-1306.

Cho, M. and Parmerter, R.R. (1992), "An efficient higher-order plate theory for laminated composites", *Compos. Struct.*, **20**(2), 113-123.

Di Sciuva, M. (1986), "Bending, vibration and buckling of simply supported thick multilayered orthotropic plates: an evaluation of a new displacement model", *J. Sound Vib.*, **105**(3), 425-442.

Dvorkin, E.N. and Bathe, K.J. (1984), "A continuum mechanics based four-node shell element for general non-linear analysis", *Eng. Comput.*, **1**(1), 77-88.

Folie, G. (1970), "Bending of clamped orthotropic sandwich plates", *J. Eng. Mech. Div.*, **96**(3), 243-265.

Grover, N., Maiti, D. and Singh, B. (2013), "A new inverse hyperbolic shear deformation theory for static and buckling analysis of laminated composite and sandwich plates", *Compos. Struct.*, **95**, 667-675.

Ha, K. (1990), "Finite element analysis of sandwich plates: an overview", *Comput. Struct.*, **37**(4), 397-403.

Huang, H. and Hinton, E. (1984), "A nine node Lagrangian Mindlin plate element with enhanced shear interpolation", *Eng. Comput.*, **1**(4), 369-379.

Kabir, H.R.H. (1995), "A shear-locking free robust isoparametric three-node triangular finite element for moderately-thick and thin arbitrarily laminated plates", *Comput. Struct.*, **57**(4), 589-597.

Kant, T. (1982), "Numerical analysis of thick plates", *Comput. Meth. Appl. Mech. Eng.*, **31**(1), 1-18.

Kant, T. and Kommineni, J. (1992), "C^0 Finite element geometrically non-linear analysis of fibre reinforced composite and sandwich laminates based on a higher-order theory", *Comput. Struct.*, **45**(3), 511-520.

Kant, T. and Swaminathan, K. (2000), "Estimation of transverse/interlaminar stresses in laminated composites-a selective review and survey of current developments", *Compos. Struct.*, **49**(1), 65-75.

Kant, T. and Swaminathan, K. (2002), "Analytical solutions for the static analysis of laminated composite and sandwich plates based on a higher order refined theory", *Compos. Struct.*, **56**(4), 329-344.

Kapuria, S. and Kulkarni, S. (2007), "An improved discrete Kirchhoff quadrilateral element based on third-order zigzag theory for static analysis of composite and sandwich plates", *Int. J. Numer. Meth. Eng.*, **69**(9), 1948-1981.

Khandan, R., Noroozi, S., Sewell, P. and Vinney, J. (2012), "The development of laminated composite plate theories: a review", *J. Mater. Sci.*, **47**(16), 5901-5910.

Khandelwal, R., Chakrabarti, A. and Bhargava, P. (2013), "An efficient FE model based on combined theory for the analysis of soft core sandwich plate", *Comput. Mech.*, **51**(5), 673-697.

Khatua, T. and Cheung, Y. (1973), "Bending and vibration of multilayer sandwich beams and plates", *Int. J. Numer. Meth. Eng.*, **6**(1), 11-24.

Kheirikhah, M.M., Khalili, S.M.R. and Malekzadeh Fard, K. (2012), "Biaxial buckling analysis of soft-core composite sandwich plates using improved high-order theory", *Euro. J. Mech. A/Solid.*, **31**(1), 54-66.

Kirchhoff, G. (1850), "Über das gleichgewicht und die bewegung einer elastischen scheibe", *J. Für Die Reine und Angewandte Mathematik*,**40**, 51-88.

Kulkarni, S. and Kapuria, S. (2007), "A new discrete Kirchhoff quadrilateral element based on the third-order theory for composite plates", *Comput. Mech.*, **39**(3), 237-246.

Lee, L. and Fan, Y. (1996), "Bending and vibration analysis of composite sandwich plates", *Comput. Struct.*, **60**(1), 103-112.

Lee, S. (2004), "Free vibration analysis of plates by using a four-node finite element formulated with assumed natural transverse shear strain", *J. Sound Vib.*, **278**(3), 657-684.

Lee, S.J. and Kim, H.R. (2013), "FE analysis of laminated composite plates using a higher order shear deformation theory with assumed strains", *Latin Am. J. Solid. Struct.*, **10**(3), 523-547.

Librescu, L. (1975), *Elastostatics and Kinetics of Anisotropic and Heterogeneous Shell-type Structures*, Noordhoff, Leyden, Netherlands

Linke, M., Wohlers, W. and Reimerdes, H.G. (2007), "Finite element for the static and stability analysis of sandwich plates", *J. Sandw. Struct. Mater.*, **9**(2), 123-142.

Liou, W.J. and Sun, C. (1987), "A three-dimensional hybrid stress isoparametric element for the analysis of laminated composite plates", *Comput. Struct.*, **25**(2), 241-249.

Lo, K., Christensen, R. and Wu, E. (1977a), "A high-order theory of plate deformation-Part 1: Homogeneous plates", *J. Appl. Mech.*, **44**(4), 663-668.

Lo, K., Christensen, R. and Wu, E. (1977b), "A high-order theory of plate deformation-part 2: laminated plates", *J. Appl. Mech.*, **44**(4), 669-676.

Manjunatha, B. and Kant, T. (1993), "On evaluation of transverse stresses in layered symmetric composite

and sandwich laminates under flexure", *Eng. Comput.*, **10**(6), 499-518.
Mantari, J., Oktem, A. and Guedes Soares, C. (2012), "A new trigonometric layerwise shear deformation theory for the finite element analysis of laminated composite and sandwich plates", *Comput. Struct.*, **94**, 45-53.
Maturi, D.A., Ferreira, A.J.M., Zenkour, A.M. and Mashat, D.S. (2014), "Analysis of sandwich plates with a new layerwise formulation", *Compos. Part B: Eng.*, **56**(0), 484-489.
Murakami, H. (1986), "Laminated composite plate theory with improved in-plane responses", *J. Appl. Mech.*, **53**(3), 661-666.
Nayak, A., Moy, S. and Shenoi, R. (2002), "Free vibration analysis of composite sandwich plates based on Reddy's higher-order theory", *Compos. Part B: Eng.*, **33**(7), 505-519.
Nayak, A., Moy, S.J. and Shenoi, R. (2003), "Quadrilateral finite elements for multilayer sandwich plates", *J. Strain Anal. Eng. Des.*, **38**(5), 377-392.
Nemeth, M.P. (2012), *Cubic zig-zag enrichment of the classical Kirchhoff kinematics for laminated and sandwich plate*, National Aeronautics and Space Administration, Langley Research Center.
Noor, A.K. and Burton, W.S. (1990), "Three-dimensional solutions for antisymmetrically solutions for antisymmetrically laminated anisotropic plates", *J. Appl. Mech.*, **57**(1), 182-188.
Noor, A.K., Burton, W.S. and Bert, C.W. (1996), "Computational models for sandwich panels and shells", *Appl. Mech. Rev.*,**49**, 155.
Oskooei, S. and Hansen, J. (2000), "Higher-order finite element for sandwich plates", *AIAA J.*, **38**(3), 525-533.
Ounis, H., Tati, A. and Benchabane, A. (2014), "Thermal buckling behavior of laminated composite plates: a finite-element study", *Front. Mech. Eng.*, **9**(1), 41-49..
Pagano, N. (1969), "Exact solutions for composite laminates in cylindrical bending", *J. Compos. Mater.*, **3**(3), 398-411.
Pagano, N. (1970), "Exact solutions for rectangular bidirectional composites and sandwich plates", *J. Compos. Mater.*, **4**(1), 20-34.
Pandit, M., Sheikh, A.H. and Singh, B.N. (2010), "Analysis of laminated sandwich plates based on an improved higher order zigzag theory", *J. Sandw. Struct. Mater.*, **12**(3), 307-326.
Pandit, M.K., Sheikh, A.H. and Singh, B.N. (2008), "An improved higher order zigzag theory for the static analysis of laminated sandwich plate with soft core", *Finite Elem. Anal. Des.*, **44**(9), 602-610.
Pandya, B. and Kant, T. (1988), "Higher-order shear deformable theories for flexure of sandwich plates-finite element evaluations", *Int. J. Solid. Struct.*, **24**(12), 1267-1286.
Plagianakos, T.S. and Saravanos, D.A. (2009), "Higher-order layerwise laminate theory for the prediction of interlaminar shear stresses in thick composite and sandwich composite plates", *Compos. Struct.*, **87**(1), 23-35.
Ramesh, S.S., Wang, C., Reddy, J. and Ang, K. (2009), "A higher-order plate element for accurate prediction of interlaminar stresses in laminated composite plates", *Compos. Struct.*, **91**(3), 337-357.
Ramtekkar, G., Desai, Y. and Shah, A. (2002), "Mixed finite-element model for thick composite laminated plates", *Mech. Adv. Mater. Struct.*, **9**(2), 133-156.
Ramtekkar, G., Desai, Y. and Shah, A. (2003), "Application of a three-dimensional mixed finite element model to the flexure of sandwich plate", *Comput. Struct.*, **81**(22), 2183-2198.
Reddy, J., Khdeir, A. and Librescu, L. (1987), "Lévy type solutions for symmetrically laminated rectangular plates using first-order shear deformation theory", *J. Appl. Mech.*, **54**(3), 740-742.
Reddy, J. and Robbins, D. (1994), "Theories and computational models for composite laminates", *Appl. Mech. Rev.*, **47**, 147.
Reddy, J.N. (1984), "A simple higher-order theory for laminated composite plates", *J. Appl. Mech.*, **51**(4), 745-752.
Reddy, J.N. (1987), "A generalization of two-dimensional theories of laminated composite plates", *Commun. Appl. Numer. Meth.*, **3**(3), 173-180.
Reddy, J.N. (1993), "An evaluation of equivalent-single-layer and layerwise theories of composite laminates", *Compos. Struct.*, **25**(1-4), 21-35.

Reissner, E. (1975), “On transverse bending of plates, including the effect of transverse shear deformation”, *Int. J. Solid. Struct.*, **11**(5), 569-573.
Rezaiee-Pajand, M., Shahabian, F. and Tavakoli, F. (2012) “A new higher-order triangular plate bending element for the analysis of laminated composite and sandwich plates”, *Struct. Eng. Mech.*, **43**(2), 253-271.
Robbins, D.H., Jr., Reddy, J.N. and Rostam-Abadi, F. (2005), “Layerwise modeling of progressive damage in fiber-reinforced composite laminates”, *Int. J. Mech. Mater. Des.*, **2**(3-4), 165-182.
Sahoo, R. and Singh, B.N. (2013), “A new inverse hyperbolic zigzag theory for the static analysis of laminated composite and sandwich plates”, *Compos. Struct.*, **105**(0), 385-397.
Sheikh, A.H. and Chakrabarti, A. (2003), “A new plate bending element based on higher-order shear deformation theory for the analysis of composite plates”, *Finite Elem. Anal. Des.*, **39**(9), 883-903.
Singh, S.K., Chakrabarti, A., Bera, P. and Sony, J. (2011), “An efficient C^0 FE model for the analysis of composites and sandwich laminates with general layup”, *Latin Am. J. Solid. Struct.*, **8**(2), 197-212.
Spilker, R. (1982), “Hybrid-stress eight-node elements for thin and thick multilayer laminated plates”, *Int. J. Numer. Meth. Eng.*, **18**(6), 801-828.
Srinivas, S. and Rao, A. (1971), “A three-dimensional solution for plates and laminates”, *J. Franklin Inst.*, **291**(6), 469-481.
Stavsky, Y. (1965), “On the theory of symmetrically heterogeneous plates having the same thickness variation of the elastic moduli”, *Top. Appl. Mech.*,**105**.
Topdar, P., Sheikh, A.H. and Dhang, N. (2003), “Finite element analysis of composite and sandwich plates using a continuous inter-laminar shear stress model”, *J. Sandw. Struct. Mater.*, **5**(3), 207-231.
Tu, T.M., Thach, L.N. and Quoc, T.H. (2010), “Finite element modeling for bending and vibration analysis of laminated and sandwich composite plates based on higher-order theory”, *Comput. Mater. Sci.*, **49**(4), S390-S394.
Whitney, J. (1970), “The effect of boundary conditions on the response of laminated composites”, *J. Compos. Mater.*, **4**(2), 192-203.
Whitney, J. and Pagano, N. (1970), “Shear deformation in heterogeneous anisotropic plates”, *J. Appl. Mech.*, **37**(4), 1031-1036.
Wu, C.P. and Hsu, C.S. (1993), “A new local high-order laminate theory”, *Compos. Struct.*, **25**(1), 439-448.
Wu, C.P. & Lin, C.C. (1993), “Analysis of sandwich plates using a mixed finite element”, *Compos. Struct.*, **25**(1), 397-405.
Xiaohui, R., Wanji, C. and Zhen, W. (2012), “A C0-type zig–zag theory and finite element for laminated composite and sandwich plates with general configurations”, *Arch. Appl. Mech.*, **82**(3), 391-406.
Zhang, Y. and Yang, C. (2009), “Recent developments in finite element analysis for laminated composite plates”, *Compos. Struct.*, **88**(1), 147-157.

CC

Appendix A

The components of strain–displacement matrices for the core and the face sheets (top- bottom) are given by

• *Core*

$$\left[B_{\chi}^{(1)}\right]=\begin{bmatrix} 0 & 0 & 0 & \frac{\partial N_i}{\partial x} & 0 & 0 & 0 & 0 & 0 & 0 & 0 & 0 & 0 \\ 0 & 0 & 0 & 0 & \frac{\partial N_i}{\partial y} & 0 & 0 & 0 & 0 & 0 & 0 & 0 & 0 \\ 0 & 0 & 0 & \frac{\partial N_i}{\partial y} & \frac{\partial N_i}{\partial x} & 0 & 0 & 0 & 0 & 0 & 0 & 0 & 0 \end{bmatrix}$$

$$\left[B_{\chi}^{(2)}\right]=\begin{bmatrix} 0 & 0 & 0 & 0 & 0 & \frac{\partial N_i}{\partial x} & 0 & 0 & 0 & 0 & 0 & 0 & 0 \\ 0 & 0 & 0 & 0 & 0 & 0 & \frac{\partial N_i}{\partial y} & 0 & 0 & 0 & 0 & 0 & 0 \\ 0 & 0 & 0 & 0 & 0 & \frac{\partial N_i}{\partial y} & \frac{\partial N_i}{\partial x} & 0 & 0 & 0 & 0 & 0 & 0 \end{bmatrix}$$

$$\left[B_{\chi}^{(3)}\right]=\begin{bmatrix} 0 & 0 & 0 & 0 & 0 & 0 & 0 & \frac{\partial N_i}{\partial x} & 0 & 0 & 0 & 0 & 0 \\ 0 & 0 & 0 & 0 & 0 & 0 & 0 & 0 & \frac{\partial N_i}{\partial y} & 0 & 0 & 0 & 0 \\ 0 & 0 & 0 & 0 & 0 & 0 & 0 & \frac{\partial N_i}{\partial y} & \frac{\partial N_i}{\partial x} & 0 & 0 & 0 & 0 \end{bmatrix}$$

$$\left[B_{\gamma_s}^{(0)}\right]=\begin{bmatrix} 0 & 0 & \frac{\partial N_i}{\partial x} & N_i & 0 & 0 & 0 & 0 & 0 & 0 & 0 & 0 & 0 \\ 0 & 0 & \frac{\partial N_i}{\partial y} & 0 & N_i & 0 & 0 & 0 & 0 & 0 & 0 & 0 & 0 \end{bmatrix}$$

$$\left[B_{\chi_s}^{(1)}\right]=\begin{bmatrix} 0 & 0 & 0 & 0 & 0 & 2N_i & 0 & 0 & 0 & 0 & 0 & 0 & 0 \\ 0 & 0 & 0 & 0 & 0 & 0 & 2N_i & 0 & 0 & 0 & 0 & 0 & 0 \end{bmatrix}$$

$$\left[B_{\chi_s}^{(2)}\right]=\begin{bmatrix} 0 & 0 & 0 & 0 & 0 & 0 & 0 & 3N_i & 0 & 0 & 0 & 0 & 0 \\ 0 & 0 & 0 & 0 & 0 & 0 & 0 & 0 & 3N_i & 0 & 0 & 0 & 0 \end{bmatrix}$$

• *Top face sheet*

$$\left[B_m^t\right]=\begin{bmatrix} 0 & 0 & 0 & c\frac{\partial N_i}{\partial x} & 0 & d\frac{\partial N_i}{\partial x} & 0 & e\frac{\partial N_i}{\partial x} & 0 & f\frac{\partial N_i}{\partial x} & 0 & 0 & 0 \\ 0 & 0 & 0 & 0 & c\frac{\partial N_i}{\partial y} & 0 & d\frac{\partial N_i}{\partial y} & 0 & e\frac{\partial N_i}{\partial y} & 0 & f\frac{\partial N_i}{\partial y} & 0 & 0 \\ 0 & 0 & 0 & c\frac{\partial N_i}{\partial y} & c\frac{\partial N_i}{\partial x} & d\frac{\partial N_i}{\partial y} & d\frac{\partial N_i}{\partial x} & e\frac{\partial N_i}{\partial y} & e\frac{\partial N_i}{\partial x} & f\frac{\partial N_i}{\partial y} & f\frac{\partial N_i}{\partial x} & 0 & 0 \end{bmatrix}$$

$with:$

$$c=\frac{h_c}{2},\quad d=\frac{h_c^2}{4},\quad e=\frac{h_c^3}{8},\quad f=\frac{h_c}{2}$$

$$\left[B_f^t\right]=\begin{bmatrix} 0 & 0 & 0 & 0 & 0 & 0 & 0 & 0 & 0 & \frac{\partial N_i}{\partial x} & 0 & 0 & 0 \\ 0 & 0 & 0 & 0 & 0 & 0 & 0 & 0 & 0 & 0 & \frac{\partial N_i}{\partial y} & 0 & 0 \\ 0 & 0 & 0 & 0 & 0 & 0 & 0 & 0 & 0 & \frac{\partial N_i}{\partial y} & \frac{\partial N_i}{\partial x} & 0 & 0 \end{bmatrix}$$

$$\left[B_c^t\right]=\begin{bmatrix} 0 & 0 & \frac{\partial N_i}{\partial x} & 0 & 0 & 0 & 0 & 0 & 0 & N_i & 0 & 0 & 0 \\ 0 & 0 & \frac{\partial N_i}{\partial y} & 0 & 0 & 0 & 0 & 0 & 0 & 0 & N_i & 0 & 0 \end{bmatrix}$$

• *Bottom face sheet*

$$\left[B_m^b\right]=\begin{bmatrix} 0 & 0 & 0 & f\frac{\partial N_i}{\partial x} & 0 & d\frac{\partial N_i}{\partial x} & 0 & h\frac{\partial N_i}{\partial x} & 0 & 0 & 0 & c\frac{\partial N_i}{\partial x} & 0 \\ 0 & 0 & 0 & 0 & f\frac{\partial N_i}{\partial y} & 0 & d\frac{\partial N_i}{\partial y} & 0 & h\frac{\partial N_i}{\partial y} & 0 & 0 & 0 & c\frac{\partial N_i}{\partial y} \\ 0 & 0 & 0 & f\frac{\partial N_i}{\partial y} & f\frac{\partial N_i}{\partial x} & d\frac{\partial N_i}{\partial y} & d\frac{\partial N_i}{\partial x} & h\frac{\partial N_i}{\partial y} & h\frac{\partial N_i}{\partial x} & 0 & 0 & c\frac{\partial N_i}{\partial y} & c\frac{\partial N_i}{\partial x} \end{bmatrix}$$

$with:$

$$f=-\frac{h_c}{2},\quad d=\frac{h_c^2}{4},\quad h=-\frac{h_c^3}{8},\quad c=\frac{h_c}{2} \tag{27}$$

$$\left[B_f^b\right]=\begin{bmatrix} 0 & 0 & 0 & 0 & 0 & 0 & 0 & 0 & 0 & 0 & 0 & \dfrac{\partial N_i}{\partial x} & 0 \\ 0 & 0 & 0 & 0 & 0 & 0 & 0 & 0 & 0 & 0 & 0 & 0 & \dfrac{\partial N_i}{\partial y} \\ 0 & 0 & 0 & 0 & 0 & 0 & 0 & 0 & 0 & 0 & 0 & \dfrac{\partial N_i}{\partial y} & \dfrac{\partial N_i}{\partial x} \end{bmatrix}$$

$$\left[B_c^b\right]=\begin{bmatrix} 0 & 0 & \dfrac{\partial N_i}{\partial x} & 0 & 0 & 0 & 0 & 0 & 0 & 0 & 0 & N_i & 0 \\ 0 & 0 & \dfrac{\partial N_i}{\partial y} & 0 & 0 & 0 & 0 & 0 & 0 & 0 & 0 & 0 & N_i \end{bmatrix}$$